Drum-Boiler Dynamics

Åström, Karl Johan; Bell, Rodney D.

1998

Document Version:
Publisher's PDF, also known as Version of record

ISSN 0280–5316
ISRN LUTFD2/TFRT--7577--SE

Drum-Boiler Dynamics

K.J. Åström
R.D. Bell

Department of Automatic Control
Lund Institute of Technology
September 1998

Department of Automatic Control
Lund Institute of Technology
Box 118
S-221 00 Lund Sweden

Document name
Internal Report

Date of issue
September 1998

Document Number
ISRN LUTFD2/TFRT--7577--SE

Author(s)
K.J. Åström and R.D. Bell

Supervisor

Sponsoring organisation
Sydkraft, NUTEK

Title and subtitle
Drum-Boiler Dynamics

Abstract

This paper describes a nonlinear dynamic model for natural circulation drum-boilers. The nonlinear model which is intended for model based control focuses on the complicated dynamics of the drum, downcomer, and riser components. A strong effort has been made to strike a balance between fidelity and simplicity. The model is derived from first principles, and is characterized by a few physical parameters. Results from validation of the model against unique plant data are presented. The model captures the shrink and swell effect very well. It also describes the behavior of the system over a wide operating range.

Key words
Drum-boiler, shrink and swell, level dynamics, pressure dynamics, two-phase flow, physical modeling, plant experiments, model validation, natural circulation.

Classification system and/or index terms (if any)

Supplementary bibliographical information

ISSN and key title
0280–5316

ISBN

Language
English

Number of pages
38

Recipient's notes

Security classification

Drum-Boiler Dynamics

K. J. Åström

Department of Automatic Control
Lund Institute of Technology
Box 118
S-221 00 Lund, Sweden
Phone: +46-46 222 8781, Fax: +46-46 138118
Email: kja@control.lth.se

R. D. Bell

Department of Computing
School of Mathematics, Physics, Computing and Electronics
Macquarie University
New South Wales 2109, Australia
Phone: +61-2 9850 9543, Fax: +61-2 9850 9551
Email: rod@mpce.mq.edu.au

Abstract This paper describes a nonlinear dynamic model for natural circulation drum-boilers. The nonlinear model which is intended for model based control focuses on the complicated dynamics of the drum, downcomer, and riser components. A strong effort has been made to strike a balance between fidelity and simplicity. The model is derived from first principles, and is characterized by a few physical parameters. Results from validation of the model against unique plant data are presented. The model captures the shrink and swell effect very well. It also describes the behavior of the system over a wide operating range.

Keywords Drum-boiler, shrink and swell, level dynamics, pressure dynamics, two-phase flow, physical modeling, plant experiments, model validation, natural circulation.

1. Introduction

There are dramatic changes in the power industry because of the deregulation. One consequence of this is that the demands for rapid changes in power generation is increasing. This leads to more stringent requirements on the control systems for the processes. It is required to keep the processes operating well for large changes in the operating conditions. One way to

achieve this is to incorporate more process knowledge into the the systems. There has also been a significant development of methods for model based control see, [24], [49] and [39]. Lack of good nonlinear process models is a bottleneck for using model based controllers. For many industrial processes there are good static models used for process design and steady state operation. By using system identification techniques it is possible to obtain black box models of reasonable complexity that describe the system well in specific operating conditions. Neither static models nor black box models are suitable for model based control. Static design models are are quite complex and they do not capture dynamics. Black box models are only valid for specific operating conditions.

This paper presents a nonlinear model for steam generation systems which are a crucial part of most power plants. The goal is to develop moderately complex nonlinear models that capture the key dynamical properties over a wide operating range. The models are based on physical principles and have a small number of parameters; most of which are determined from construction data. Particular attention has been devoted to model drum level dynamics well. Drum level control is an important problem for nuclear as well as conventional plants, see [32], [1]. In [45] it is stated that up to 13% of all reactor trips in France in 1983 were attributed to steam generator control problems. One reason is that the control problem is difficult because of the complicated shrink and swell dynamics. This creates a non-minimum phase behavior which changes significantly with the operating conditions.

Since boilers are so common there are many modeling efforts. There are complicated models in the form of large simulation codes which are based on finite element approximations to partial differential equations. Although such models are important for plant design, simulators and commissioning they are of little interest for control design because of their complexity. Among the early work on models suitable for control we can mention [47], [16], [48], [17], [44], [54], [50], [14], [57], [31], [41], [51], [53], [19], [31], [40], [21], [7] [4], [9], [3], [13], [2], [33], [55], [11], [43]. Boiler modeling is still of substantial interest. Among more recent publications we can mention [35], [36], [29], [28], [56], [32], [37].

The work presented in this paper is part of an ongoing long range research project that started with [21] and [9]. The work has been a mixture of physical modeling, system identification and model simplification. It has been guided by plant experiments in Sweden and Australia. The unique measurements reported in [21] have been particularly useful. A sequence of experiments with much excitation were performed on a boiler over a wide range of operating conditions. Because of the excitation used, these measurements reveal much of the dynamics of interest for control. Results of system identification experiments indicated that the essential dynamics could in fact be captured by a simple models [7]. However, it has not been easy to find first principles models of the appropriate complexity. Many different approaches have been used. We have searched for the physical phenomena that yield models of the appropriate complexity. Over the years the models have changed in complexity both increasing and decreasing; empirical coefficients have been replaced by physical parameters as our understanding of the system has increased. The papers [7], [8], [5], [6], [10] describe how the models have evolved. The models have also been used for control design, see [42], [46] and [15]. Models based on a similar structure

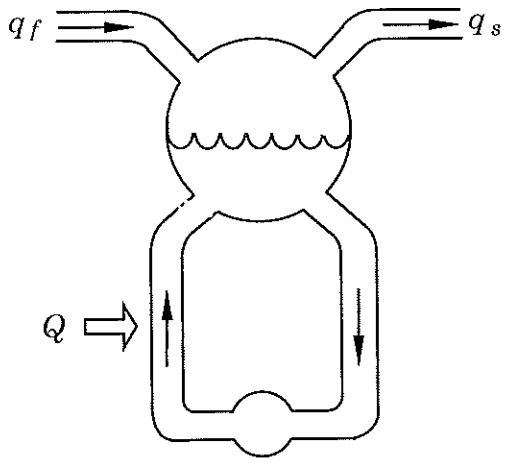

Figure 1 Schematic picture of the boiler.

have been used for Deaerator simulation and control [34] and for nuclear reactors [58], [27].

2. Global Mass and Energy Balances

A schematic picture of a boiler system is shown in Figure 1. The heat, Q, supplied to the risers causes boiling. Gravity forces the saturated steam to rise causing a circulation in the riser-drum-downcomer loop. Feedwater, q_f, is supplied to the drum and saturated steam, q_s, is taken from the drum to the superheaters and the turbine. The presence of steam below the liquid level in the drum causes the shrink-and-swell phenomenon which makes level control difficult. In reality the system is much more complicated than shown in the figure. The system has a complicated geometry and there are many downcomer and riser tubes. In spite of the complexity of the system it turns out that its gross behavior is well captured by global mass and energy balances.

A key property of boilers is that there is a very efficient heat transfer due to boiling and condensation. All parts of the system which are in contact with the saturated liquid-vapor mixture will be in thermal equilibrium. Energy stored in steam and water is released or absorbed very rapidly when the pressure changes. This mechanism is the key for understanding boiler dynamics. The rapid release of energy ensures that different parts of the boiler change their temperature in the same way. For this reason the dynamics can be captured by models of low order. Drum pressure and power dynamics can in fact be represented very well with first order dynamics as shown in [7]. At first it id surprising that the distributed effects can be neglected for a system with so large physical dimensions.

Typical values of stored energy for two different boilers are given in Table 1. The P16-G16 plant is a 160MW unit in Sweden and the Eraring plant is a 660MW unit in Australia. The ratio of the energy stored in the metal to that stored in the water is approximately 1 for P16-G16 and 4 for the Eraring unit. These figures agree well with the fact that the metal mass scales as $P^{1.5}$, where P is electric power.

The numbers in Table 1 also give a measure of the time it takes to

Table 1 Energy stored in metal, water and steam for two boilers operating at rated pressure and temperature but at different power generation conditions. The values are normalized with the power at the operating conditions. The unit is J/W=s, the entries can thus be interpreted as constants for the different storage mechanisms.

Boiler	*Operating Condition*	*Metal*	*Water*	*Steam*	*Total*
P16-G16	80MW	641	739	64	1444
P16-G16	160MW	320	333	37	690
Eraring	330MW	1174	303	60	1537
Eraring	660MW	587	137	35	759

deplete the stored energy at the generated rate. Although the total normalized stored energy is approximately the same for both plants there is a considerable reduction proportionally in the stored energy in the water for the larger plant. This results in larger variations in water level for the larger plant under proportionally similar operating condition changes. This implies that the level control problem is more difficult for large boilers.

Balance Equations

Much of the behavior of the system is captured by global mass and energy balances. Let the inputs to the system be the heat flow rate to the risers, Q, the feedwater mass flow rate, q_f, and the steam mass flow rate, q_s. Furthermore, let the outputs of the system be drum pressure, p, and drum water level, ℓ.

To write the equations, let V denote volume, ρ denotes specific density, u specific internal energy, h specific enthalpy, t temperature and q mass flow rate. Furthermore let subscripts s, w, f and m refer to steam, water, feedwater and metal respectively. Sometimes, for clarification, we need a notation for the system components. For this purpose we will use double subscripts where t denotes total system, d drum and r risers. The metal's specific heat is C_p and m_t is the total mass for the metal tubes and drum.

The global mass balance is

$$\frac{d}{dt}\left[\rho_s V_{st} + \rho_w V_{wt}\right] = q_f - q_s, \tag{1}$$

and the global energy balance is

$$\frac{d}{dt}\left[\rho_s u_s V_{st} + \rho_w u_w V_{wt} + m_t C_p t_m\right] = Q + q_f h_f - q_s h_s. \tag{2}$$

Let v be the specific volume. The internal energy is then given by

$$u = h - pv. \tag{3}$$

The global energy balance can then be written as

$$\frac{d}{dt}\left[\rho_s h_s V_{st} + \rho_w h_w V_{wt} - pV_t + m_t C_p t_m\right] = Q + q_f h_f - q_s h_s, \tag{4}$$

where V_{st} and V_{wt} represent the total steam and water volumes respectively. The total volume of the drum, downcomer and risers, V_t, is constant and is given by,

$$V_t = V_{st} + V_{wt}. \tag{5}$$

The metal temperature t_m can be expressed as a function of pressure by assuming that t_m is equal to the saturation temperature of steam t_s which corresponds to p. The right hand side of equation (4) represents the energy flow to the system from fuel and feedwater and the energy flow from the system via the steam.

A Second Order Model

Equations (1), (4) and (5) combined with saturated steam tables yields a simple boiler model. Mathematically the model is a differential algebraic system. Such systems can be entered directly in modeling languages such as Omola and it can be simulated directly using Omsim, see [38]. In this way we avoid making manual operations which are time consuming and error prone.

We will, however, make manipulations of the model to obtain a state model. This gives insight into the key physical mechanisms that affect the dynamic behavior of the system. There are many possible choices of state variables. Since all parts are in thermal equilibrium it is natural to choose drum pressure p as one state variable. This variable is also easy to measure. Using saturated steam tables, the variables ρ_s, ρ_w, h_s and h_w can then be expressed as functions of steam pressure. The second state variable can be chosen as the total volume of water in the system, i.e. V_{wt}. Using Equation (5) and noting that V_t is constant, V_{st} can then be eliminated from Equations (1) and (4) to give the following state equations,

$$\begin{aligned} e_{11}\frac{dV_{wt}}{dt} + e_{12}\frac{dp}{dt} &= q_f - q_s \\ e_{21}\frac{dV_{wt}}{dt} + e_{22}\frac{dp}{dt} &= Q + q_f h_f - q_s h_s, \end{aligned} \tag{6}$$

where

$$\begin{aligned} e_{11} &= \rho_w - \rho_s \\ e_{12} &= V_{st}\frac{\partial \rho_s}{\partial p} + V_{wt}\frac{\partial \rho_w}{\partial p} \\ e_{21} &= \rho_w h_w - \rho_s h_s \\ e_{22} &= V_{st}(h_s\frac{\partial \rho_s}{\partial p} + \rho_s\frac{\partial h_s}{\partial p}) + V_{wt}(h_w\frac{\partial \rho_w}{\partial p} + \rho_w\frac{\partial h_w}{\partial p}) - V_t + m_t C_p\frac{\partial t_s}{\partial p}. \end{aligned} \tag{7}$$

This model captures the gross behavior of the boiler quite well. In particular it describes the response of drum pressure to changes in input power, feedwater flow rate and steam flow rate very well. The model does, however, have one serious deficiency. Although it describes the total water in the system it does not capture the behavior of the drum level because it does not describe the distribution of steam and water in the system.

Table 2 Numerical values of the terms of the coefficient e_1 at normal operating pressure.

Boiler	*Power*	$h_c V_{st} \frac{\partial \rho_s}{\partial p}$	$\rho_s V_{st} \frac{\partial h_s}{\partial p}$	$\rho_w V_{wt} \frac{\partial h_w}{\partial p}$	$m_t C_p \frac{\partial t_s}{\partial p}$	V_t
P16-G16	80MW	360	-40	2080	1410	85
P16-G16	160MW	420	-40	1870	1410	85
Eraring	330MW	700	-270	2240	4620	169
Eraring	660MW	810	-270	2020	4620	169

Further Simplifications

Additional simplifications can be made if we are only interested in the drum pressure. Multiplying (1) by h_w and subtracting the result from (4) gives

$$h_c \frac{d}{dt}(\rho_s V_{st}) + \rho_s V_{st} \frac{dh_s}{dt} + \rho_w V_{wt} \frac{dh_w}{dt} - V_t \frac{dp}{dt} + m_t C_p \frac{dt_s}{dt} = Q - q_f (h_w - h_f) - q_s h_c,$$

where $h_c = h_s - h_w$ is the condensation enthalpy.

If the drum level is controlled well the variations in the steam volume are small. Neglecting these variations we get the following approximate model.

$$e_1 \frac{dp}{dt} = Q - q_f(h_w - h_f) - q_s h_c, \tag{8}$$

where

$$e_1 = h_c V_{st} \frac{\partial \rho_s}{\partial p} + \rho_s V_{st} \frac{\partial h_s}{\partial p} + \rho_w V_{wt} \frac{\partial h_w}{\partial p} + m_t C_p \frac{\partial t_s}{\partial p} - V_t.$$

The term V_t in e_1 comes from the relation between internal energy and enthalpy. This term is often neglected in modeling, see [18]. The relative magnitudes of the terms of e_1 for two boilers are given in Table 2. The terms containing $\partial h_w/\partial p$ and $\partial t_s/\partial p$ are the dominating terms in the expression for e_1. This implies that the changes in energy content of the water and metal masses are the physical phenomena that dominate the dynamics of drum pressure. A good approximation of e_1 is

$$e_1 \approx \rho_w V_{wt} \frac{\partial h_w}{\partial p} + m C_p \frac{\partial t_s}{\partial p}.$$

Table 2 gives good insight into the physical mechanisms that govern the behavior of the system. Consider for example the situation when the pressure changes. The change in stored energy for this pressure change will be proportional to the numbers in the last two columns of the table. The column for the steam $(\partial h_s/\partial p)$ indicates that energy changes in the steam are two orders of magnitude smaller than the energy changes in water

and metal. The balance of the change in energy is used in the boiling or condensation of steam. The quantity

$$q_{ct} = \frac{h_w - h_f}{h_c} q_f + \frac{1}{h_c}\left(\rho_s V_{st} \frac{\partial h_s}{\partial p} + \rho_w V_{wt} \frac{\partial h_w}{\partial p} - V_t + m_t C_p \frac{\partial t_s}{\partial p}\right) \frac{dp}{dt} \quad (9)$$

can be interpreted as the condensation flow rate. This process results in a natural feedback system that tries to maintain steam pressure irrespective of the heat energy input to the system.

The model (8) captures the responses in drum pressure to changes in heat flow rate, feedwater flow rate, feedwater temperature and steam flow rate very well. An attractive feature is that all parameters are given by steam tables and construction data. The equation gives good insight into the nonlinear characteristics of the pressure response, since both e_1 and the enthalpies on the right hand side of the equation depend on the operating pressure. To obtain a complete model for simulating the drum pressure a model for the steam valve has to be supplied.

The pressure model given by Equation (8) is similar to the models in [17], [50], [7] and [35]. Models similar to (8) are included in most boiler models. Since the model (8) is based on global mass and energy balances it cannot capture phenomena that are related to the distribution of steam and water in the boiler. Therefore it cannot cannot model the drum level.

3. Distribution of Steam in Risers and Drum

To obtain a model which can describe the behavior of the drum level we must account for the distribution of steam and water in the system. The redistribution of steam and water in the system causes the shrink-and-swell effect which causes the non-minimum-phase behavior of level dynamics, see [32]. One manifestation is that the level will increase when the steam valve is opened because the drum pressure will drop, causing a swelling of the steam bubbles below the drum level.

The behavior of two phase flow is very complicated and is typically modeled by partial differential equations, see [30] and [26]. A key contribution of this paper is that it is possible to derive relatively simple lumped parameter models that agree well with experimental data.

Saturated Mixture Quality in a Heated Tube

We will start by discussing the dynamics of water and steam in a heated tube. Consider a vertical tube with uniform heating. Let ρ be the density of the steam-water mixture. Furthermore let q be the mass flow rate, A the area of the cross section of the tube, V the volume, u the specific internal energy, and Q the heat supplied to the tube. All quantities are distributed in time, t, and space, z. Assume for simplicity that all quantities are the same in a cross section of the tube. The spatial distribution can then be captured by one coordinate z and all functions are then functions of z and time t.

The mass and energy balances for a heated section of the tube are

$$A\frac{\partial \rho}{\partial t} + \frac{\partial q}{\partial z} = 0$$
$$\frac{\partial \rho u}{\partial t} + \frac{1}{A}\frac{\partial qu}{\partial z} = \frac{Q}{V}.$$

Let α_m denote the mass fraction of steam in the flow i.e. the quality of the mixture, and let u_s and u_w denote the saturated internal energies of steam and water. The specific internal energy of the mixture of steam and water is thus

$$u = \alpha_m u_s + (1-\alpha_m)u_w = u_w + \alpha_m(u_s - u_w) = u_w + \alpha_m u_c. \tag{10}$$

In steady state we get

$$\frac{\partial q}{\partial z} = 0$$
$$\frac{\partial qu}{\partial z} = qu_c\frac{\partial \alpha_m}{\partial z} = \frac{QA}{V}.$$

The flow is thus constant and internal energy increases at a constant rate. It follows from Equation (10) that the steam-mass fraction also increases linearly, i.e.

$$\alpha_m = \frac{QA}{qu_c V}z.$$

Let ξ be a normalized length coordinate along the risers and let α_r be the steam quality at the riser outlet. The steam fraction along the tube is thus given by

$$\alpha_m(\xi) = \alpha_r\xi \quad 0 \le \xi \le 1. \tag{11}$$

A slight refinement of the model is to assume that boiling starts at a distance x_0 from the bottom of the risers. In this case the steam distribution will be characterized by two variables α_r and x_0 instead of just α_r. For the experimental data in this paper it adds very little to the prediction power of the model. For this reason we use the simpler model although the modification may be important for other boilers.

There is actually a slip between water and steam in the risers. To take this into account requires much more complicated models. The justification for neglecting this is that it does not have a major influence on the fit to experimental data.

The volume and mass fractions of steam are related through

$$\alpha_v = f(\alpha_m),$$

where

$$f(\alpha_m) = \frac{\rho_w\alpha_m}{\rho_s + (\rho_w - \rho_s)\alpha_m}. \tag{12}$$

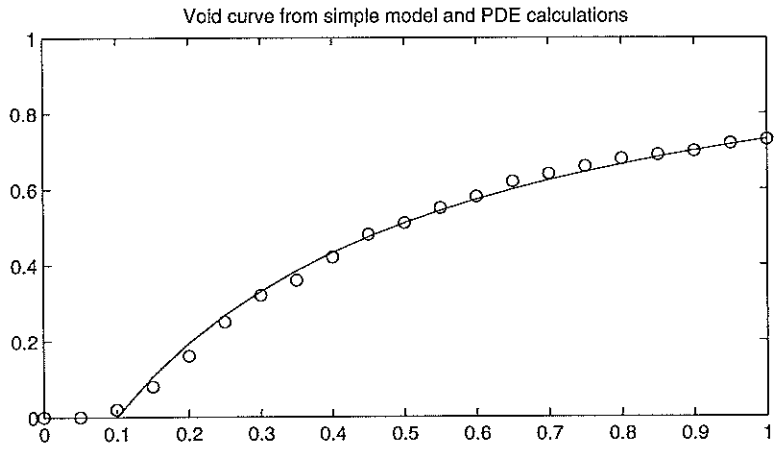

Figure 2 Comparison of steam volume distribution calculated from Equations (11) and (12) (full lines) with results of numerical solutions of detailed partial differential equation models (circles).

It has been verified that the simple model which uses a linear steam-mass fraction given by Equation (11) and a steam-volume fraction given by Equation (12) describes quite well what happens in a typical riser tube. This is illustrated in Figure 2 which compares the steam distribution in a tube computed from Equations (11) and (12) with computations from a detailed computational fluid dynamics code for a riser tube in a nuclear reactor. The complex code also takes into account that there is a slip between the flow of steam and water. It is interesting to see that the simple model captures the distribution quite well.

Average Steam Volume Ratio

To model drum level it is essential to describe the total amount of steam in the risers. This is governed by the average volume fraction in the risers. Assume that the mass fraction is linear along the riser as expressed by Equation (11) we find that the average volume fraction $\bar{\alpha}_v$ is given by

$$\begin{aligned}\bar{\alpha}_v &= \int_0^1 \alpha_v(\xi)d\xi = \frac{1}{\alpha_r}\int_0^1 f(\alpha_r\xi)d(\alpha_r\xi) = \frac{1}{\alpha_r}\int_0^{\alpha_r} f(\xi)d\xi \\ &== \frac{\rho_w}{\rho_w-\rho_s}\left(1-\frac{\rho_s}{(\rho_w-\rho_s)\alpha_r}\ell n\Big(1+\frac{\rho_w-\rho_s}{\rho_s}\alpha_r\Big)\right).\end{aligned} \tag{13}$$

A Lumped Parameter Model

Since we do not want to use partial differential equations they will be approximated using the Galerkin method. To do this it will be assumed that the steam mass quality distribution is linear, i.e. Equation (11) holds, also under dynamic conditions.

The transfer of mass and energy between steam and water by condensation and evaporation is a key element in the modeling. When modeling the phases separately the transfer must be accounted for explicitly. This can be avoided by writing joint balance equations for water and steam. The global mass balance for the riser section is

$$\frac{d}{dt}\left(\rho_s\bar{\alpha}_v V_r + \rho_w(1-\bar{\alpha}_v)V_r\right) = q_{dc} - q_r, \tag{14}$$

where q_r is the total mass flow rate out of the risers and q_{dc} is the total mass flow rate into the risers. The global energy balance for the riser section is

$$\frac{d}{dt}\left(\rho_s h_s \bar{\alpha}_v V_r + \rho_w h_w (1-\bar{\alpha}_v) V_r - pV_r + m_r C_p t_s\right) = Q + q_{dc} h_w - (\alpha_r h_c + h_w) q_r. \quad (15)$$

Circulation Flow

For a forced circulation boiler downcomer flow rate, q_{dc}, is a control variable. For a natural circulation boiler the flow rate is instead driven by the density gradients in the risers and the downcomers. The momentum balance for the downcomer riser loop is

$$(L_r + L_{dc})\frac{dq_{dc}}{dt} = (\rho_w - \rho_s)\bar{\alpha}_v V_r g - \frac{k}{2}\frac{q_{dc}^2}{\rho_w A_{dc}},$$

where k is a dimensionless friction coefficient and L_r and L_{dc} are lengths. This is a first order system with the time constant

$$T = \frac{(L_r + L_{dc})A_{dc}\rho_w}{kq_{dc}}.$$

With typical numerical values we find that the time constant is about a second. This is short in comparison with the sampling period of our experimental data which is 10 seconds and we will therefore use the steady state relation

$$\rho_w A_{dc}(\rho_w - \rho_s) g \bar{\alpha}_v V_r = \frac{1}{2} k q_{dc}^2. \quad (16)$$

Distribution of Steam in the Drum

The physical phenomena in the drum are quit complicated. Steam enters from many riser tubes, feedwater enters through a complex arrangement, water leaves through the downcomer tubes and steam through the steam valve. The geometry and the flow pattern are complicated. The basic mechanisms that occur are that feedwater is heated through condensation of the steam as steam bubbles through the water. Modeling of the drum is therefore difficult.

Let V_d be the volume under the liquid level in the drum, let the V_{sd} and V_{wd} be the volume of steam and water under the liquid level and let the steam flow rate through the liquid surface in the drum be q_{sd}. Recall that q_r is the flow rate out of the risers, q_f the feedwater flow rate and q_{dc} the downcomer flow rate. The mass balance for the steam under the water level in the drum is

$$\frac{d}{dt}(\rho_s V_{sd}) = \alpha_r q_r - q_{sd} - q_{cd} \quad (17)$$

where q_{cd} is the condensation flow which is given by

$$q_{cd} = \frac{h_w - h_f}{h_c} q_f + \frac{1}{h_c}\left(\rho_s V_{sd}\frac{dh_s}{dt} + \rho_w V_{wd}\frac{dh_w}{dt} - V_{sd} + m_d C_p \frac{dt_s}{dt}\right). \quad (18)$$

The flow rate q_{sd} is given by a momentum balance. The flow is driven by the density differences of water and steam, and the momentum of the flow entering the drum. The mechanisms are very complicated because of the complex flow pattern and the geometry of the drum. Several models of different complexity have been attempted. Good fit to the experimental data have been obtained with the following empirical model

$$q_{sd} = \frac{\rho_s}{T_d}(V_{sd} - V_{sd}^0) + \alpha_r q_{dc} + \beta(q_{dc} - \alpha_r q_r). \tag{19}$$

Here V_{sd}^0 denotes the volume of steam in the drum in the hypothetical situation when there is no condensation of steam in the drum and T_d is the residence time of the steam in the drum, which is approximated by

$$T_d = \frac{\rho_s V_{sd}^0}{q_s}. \tag{20}$$

Drum Level

Having accounted for the distribution of the steam below the drum level, we can now describe the drum level. The volume of water in the drum, V_{wd}, is given by

$$V_{wd} = V_{wt} - V_{dc} - (1 - \bar{\alpha}_v)V_r. \tag{21}$$

Let the wet surface of the drum be A_d. The deviation of the drum level ℓ measured from its normal operating level is

$$\ell = \frac{V_{wd} + V_{sd}}{A_d} = \ell_w + \ell_s. \tag{22}$$

4. The Model

Combining the results of Sections 2 and 3 we can now obtain a model that gives a good description of the boiler including the drum level. The model is given by the differential equations (1), (4), (14), (15) and (17). In addition there are a number of algebraic equations. The circulation flow rate q_{dc} is given by the static momentum balance (16), the steam flow rate through the liquid surface of the drum q_{sd} by (19) and the drum level ℓ by Equation (22). The volumes are related through Equations (5) and (21). The model is a differential algebraic system, see [25]. Since most available simulation software requires state equations we will also derive a state model. This is done by algebraic manipulations which result in explicit equations for the derivatives of the state variables.

Selection of State Variables

State variables can be chosen in many different ways. It is convenient to choose states as variables with good physical interpretation that describe storage of mass, energy and momentum. The accumulation of water is represented by the total water volume V_{wt}. The total energy is represented by the drum pressure p and the distribution of steam and water is captured by the steam-mass fraction in the risers α_r and the steam volume in the drum V_{sd}.

Pressure and Water Dynamics

State equations for pressure p and the total amount of water V_{wt} in the systems were obtained from the global mass and energy balances, Equations (1) and (4). These equations can be written as (6).

Riser Dynamics

The mass and energy balances for the risers are given by equations (14) and (15). Eliminating the flow rate out of the risers, q_r, by multiplying equation (14) by $-(h_w + \alpha_r h_c)$ and adding to Equation (15) gives,

$$\frac{d}{dt}(\rho_s h_s \bar{\alpha}_v V_r) - (h_w + \alpha_r h_c)\frac{d}{dt}(\rho_s \bar{\alpha}_v V_r) + \frac{d}{dt}(\rho_w h_w (1-\bar{\alpha}_v)V_r) - (h_w + \alpha_r h_c)\frac{d}{dt}(\rho_w (1-\bar{\alpha}_v)V_r) - V_r \frac{dp}{dt} + m_r C_p \frac{dt_s}{dt} = Q - \alpha_r h_c q_{dc}$$

This can be simplified to

$$h_c(1-\alpha_r)\frac{d}{dt}(\rho_s \bar{\alpha}_v V_r) + \rho_w (1-\bar{\alpha}_v) V_r \frac{dh_w}{dt} - \alpha_r h_c \frac{d}{dt}(\rho_w (1-\bar{\alpha}_v)V_r) + \rho_s \bar{\alpha}_v V_r \frac{dh_s}{dt} - V_r \frac{dp}{dt} + m_r C_p \frac{dt_s}{dt} = Q - \alpha_r h_c q_{dc} \tag{23}$$

If the state variables p and α_r are known the riser flow rate q_r can be computed from Equation (14). This gives

$$\begin{aligned} q_r &= q_{dc} - \frac{d}{dt}(\rho_s \bar{\alpha}_v V_r) - \frac{d}{dt}(\rho_w (1-\bar{\alpha}_v)V_r) \\ &= q_{dc} - V_r \frac{d}{dt}\big((1-\bar{\alpha}_v)\rho_w + \bar{\alpha}_v \rho_s\big) = q_{dc} - V_r \frac{d}{dt}\big(\rho_w - \bar{\alpha}_v(\rho_w - \rho_s)\big) \\ &= q_{dc} - V_r \frac{\partial}{\partial p}\big((1-\bar{\alpha}_v)\rho_w + \bar{\alpha}_v \rho_s\big)\frac{dp}{dt} + V_r(\rho_w - \rho_s)\frac{\partial \bar{\alpha}_v}{\partial \alpha_r}\frac{d\alpha_r}{dt}. \end{aligned} \tag{24}$$

Drum Dynamics

The dynamics for the steam in the drum is obtained from the mass balance (17). Introducing the expression (24) for q_r and the expression (18) for q_{cd} into this equation we find

$$\rho_s \frac{dV_{sd}}{dt} + V_{sd}\frac{d\rho_s}{dt} + \frac{1}{h_c}\Big(\rho_s V_{sd}\frac{dh_s}{dt} + \rho_w V_{wd}\frac{dh_w}{dt} - V_{sd} + m_d C_p \frac{dt_s}{dt}\Big) + \alpha_r(1+\beta)V_r \frac{d}{dt}\big((1-\bar{\alpha}_v)\rho_w + \bar{\alpha}_v \rho_s\big) = \frac{\rho_s}{T_d}(V_{sd}^0 - V_{sd}) + \frac{h_f - h_w}{h_c} q_f. \tag{25}$$

Many of the complex phenomena in the drum are captured by this equation.

Summary

The state variables are: drum pressure p, total water volume V_{wt}, quality at the riser outlet α_r, and volume of steam under the liquid level in the drum V_{sd}. The time derivatives of these variables are given by the equations (6),

(23), and (25). By straight forward but tedious calculations these equations can be rewritten as

$$\begin{aligned} e_{11}\frac{dV_{wt}}{dt} + e_{12}\frac{dp}{dt} &= q_f - q_s \\ e_{21}\frac{dV_{wt}}{dt} + e_{22}\frac{dp}{dt} &= Q + q_f h_f - q_s h_s \\ e_{32}\frac{dp}{dt} + e_{33}\frac{d\alpha_r}{dt} &= Q - \alpha_r h_c q_{dc} \\ e_{42}\frac{dp}{dt} + e_{43}\frac{d\alpha_r}{dt} + e_{44}\frac{dV_{sd}}{dt} &= \frac{\rho_s}{T_d}(V_{sd}^0 - V_{sd}) + \frac{h_f - h_w}{h_c} q_f, \end{aligned} \tag{26}$$

where the coefficients e_{ij} are given by

$$\begin{aligned} e_{11} &= \rho_w - \rho_s \\ e_{12} &= V_{wt}\frac{\partial \rho_w}{\partial p} + V_{st}\frac{\partial \rho_s}{\partial p} \\ e_{21} &= \rho_w h_w - \rho_s h_s \\ e_{22} &= V_{wt}\left(h_w\frac{\partial \rho_w}{\partial p} + \rho_w\frac{\partial h_w}{\partial p}\right) + V_{st}\left(h_s\frac{\partial \rho_s}{\partial p} + \rho_s\frac{\partial h_s}{\partial p}\right) - V_t + m_t C_p\frac{\partial t_s}{\partial p} \\ e_{32} &= \left(\rho_w\frac{\partial h_w}{\partial p} - \alpha_r h_c\frac{\partial \rho_w}{\partial p}\right)(1-\bar{\alpha}_v)V_r + \left((1-\alpha_r)h_c\frac{\partial \rho_s}{\partial p} + \rho_s\frac{\partial h_s}{\partial p}\right)\bar{\alpha}_v V_r \\ &\quad + \left(\rho_s + (\rho_w - \rho_s)\alpha_r\right)h_c V_r\frac{\partial \bar{\alpha}_v}{\partial p} - V_r + m_r C_p\frac{\partial t_s}{\partial p} \\ e_{33} &= \left((1-\alpha_r)\rho_s + \alpha_r\rho_w\right)h_c V_r\frac{\partial \bar{\alpha}_v}{\partial \alpha_r} \\ e_{42} &= V_{sd}\frac{\partial \rho_s}{\partial p} + \frac{1}{h_c}\left(\rho_s V_{sd}\frac{\partial h_s}{\partial p} + \rho_w V_{wd}\frac{\partial h_w}{\partial p} - V_{sd} + m_d C_p\frac{\partial t_s}{\partial p}\right) \\ &\quad + \alpha_r(1+\beta)V_r\left(\bar{\alpha}_v\frac{\partial \rho_s}{\partial p} + (1-\bar{\alpha}_v)\frac{\partial \rho_w}{\partial p} + (\rho_s - \rho_w)\frac{\partial \bar{\alpha}_v}{\partial p}\right) \\ e_{43} &= \alpha_r(1+\beta)(\rho_s - \rho_w)V_r\frac{\partial \bar{\alpha}_v}{\partial \alpha_r} \\ e_{44} &= \rho_s. \end{aligned} \tag{27}$$

In addition steam tables are required to evaluate h_s, h_w, ρ_s, ρ_w, $\partial\rho_s/\partial p$, $\partial\rho_w/\partial p$, $\partial h_s/\partial p$, $\partial h_w/\partial p$, t_s, and $\partial t_s/\partial p$ at the saturation pressure p. The simulation results in Sections 5 and 6 have used a quadratic function to represent the steam tables over the desired operating conditions. This has made the calculation of partial derivatives with respect to pressure particularly simple since they become a linear function. A more accurate method of table look-up with interpolation was also tried but with little difference in the response but significantly longer compute time. The particular approximations are given in the program listing in Appendix B.

The partial derivatives of volume fractions with respect to pressure and mass fractions are also required. They are obtained by differentiating

Equation (13). We get

$$\begin{aligned}\frac{\partial\bar{\alpha}_v}{\partial p} &= \frac{1}{(\rho_w-\rho_s)^2}\Big(\rho_w\frac{\partial\rho_s}{\partial p}-\rho_s\frac{\partial\rho_w}{\partial p}\Big)\Big(1+\frac{\rho_w}{\rho_s}\frac{1}{1+\eta}-\frac{\rho_s+\rho_w}{\eta\rho_s}\ell n(1+\eta)\Big)\\ \frac{\partial\bar{\alpha}_v}{\partial\alpha_r} &= \frac{\rho_w}{\rho_s\eta}\Big(\frac{1}{\eta}\ell n(1+\eta)-\frac{1}{1+\eta}\Big),\end{aligned} \tag{28}$$

where $\eta = \alpha_r(\rho_w-\rho_s)/\rho_s$. The algebraic relationships for steam volume fraction $\bar{\alpha}_v$ Equation (13), volume of water in drum V_{wd} Equation (21), drum level ℓ Equation (22), residence time T_d Equation (20), and downcomer mass flow rate q_{dc} Equation (16) complete the simulation equations. It is also of interest to know the total condensation flow q_{ct} and the flow rate out of the risers q_r. These flows are given by Equations (9) and (24), hence

$$\begin{aligned}\bar{\alpha}_v &= \frac{\rho_w}{\rho_w-\rho_s}\left(1-\frac{\rho_s}{(\rho_w-\rho_s)\alpha_r}\ell n\Big(1+\frac{\rho_w-\rho_s}{\rho_s}\alpha_r\Big)\right)\\ V_{wd} &= V_{wt}-V_{dc}-(1-\bar{\alpha}_v)V_r\\ \ell &= \frac{V_{wd}+V_{sd}}{A_d}\\ T_d &= \frac{\rho_s V_{sd}^0}{q_{sd}}\\ kq_{dc}^2 &= 2\rho_w A_{dc}(\rho_w-\rho_s)g\bar{\alpha}_v V_r\\ q_{ct} &= \frac{h_w-h_f}{h_c}q_f+\frac{1}{h_c}\Big(\rho_s V_{st}\frac{\partial h_s}{\partial p}+\rho_w V_{wt}\frac{\partial h_w}{\partial p}-V_t+m_t C_p\frac{\partial t_s}{\partial p}\Big)\frac{dp}{dt}\\ q_r &= q_{dc}-V_r\Big(\bar{\alpha}_v\frac{\partial\rho_s}{\partial p}+(1-\bar{\alpha}_v)\frac{\partial\rho_w}{\partial p}+(\rho_w-\rho_s)\frac{\partial\bar{\alpha}_v}{\partial p}\Big)\frac{dp}{dt}\\ &\quad+(\rho_w-\rho_s)V_r\frac{\partial\bar{\alpha}_v}{\partial\alpha_r}\frac{d\alpha_r}{dt}.\end{aligned}$$

Structure of the Equations

Notice that the Equation(26) has an interesting lower triangular structure where the state variables can be grouped as

$$\Big(((V_{wt},p),\alpha_r),V_{sd}\Big),$$

where the variables inside each parenthesis can be computed independently. The model can thus be regarded as a nesting of a second, a third and a fourth order model. The second order model describes drum pressure and total volume of water in the system. The equations are global mass and energy balances. There is a very weak coupling between these equations which is caused by the condensation flow. The third order model captures the steam dynamics in the risers and the fourth order model also describes the accumulation of steam below the water surface in the drum dynamics. The third equation is a combination of mass and energy balances for the riser, and the fourth equation is a mass balance for steam under the water level in the drum.

Linearizing Equation (26) shows that the system has a double pole at the origin and poles at $-h_r q_{dc}/e_{33}$ and $-T_d$.

The nested structure reflects how the model was developed. The third order model is an improved version of the models in [5] and [6]. In [10] we added drum dynamics as a fourth order model. The model in this paper is a refined version of that model. Different models of higher order have also been developed.

Parameters

An interesting feature of the model is that it requires only a few parameters to characterize the system. They are:

- Drum volume V_d
- Riser volume V_r
- Downcomer volume V_{dc}
- Drum area A_d at normal operating level
- Total metal mass m_t
- Total riser mass m_r
- Friction coefficient in downcomer-riser loop k
- Volume of steam in the drum V_{sd}^0 when there is no condensation
- Parameter β in the empirical equation (19)

A convenient way to find the k is to compute it from the circulation flow rate. Perturbation studies have shown that the behavior of the system is not very sensitive to the parameters.

The parameters used in this paper were based on construction data. Some of them were quite crude. Grey-box identification, [12] was used in a comprehensive investigation in [20] and [52]. Parameters were estimated and hypothesis testing was used to compare several model structures. The results showed that pressure dynamics can be improved significantly by increasing the metal masses. Significant improvements can also be obtained by adjusting the coefficients in the calibration formula for the sensors.

In [52] it was also shown that the friction coefficient is not identifiable from the data. There is in fact a relation between the initial steam quality and friction. A consequence of this is that it is highly desirable for accurate modeling to measure the circulation flow. This could also be an important signal to use in a level control system.

In [20] hypothesis testing was also applied to the models [5], [6] (third order), [10] (fourth order). These studies showed conclusively that the improvements obtained with the fourth order model are significant. Computations on fifth order models showed that the increased complexity could not be justified.

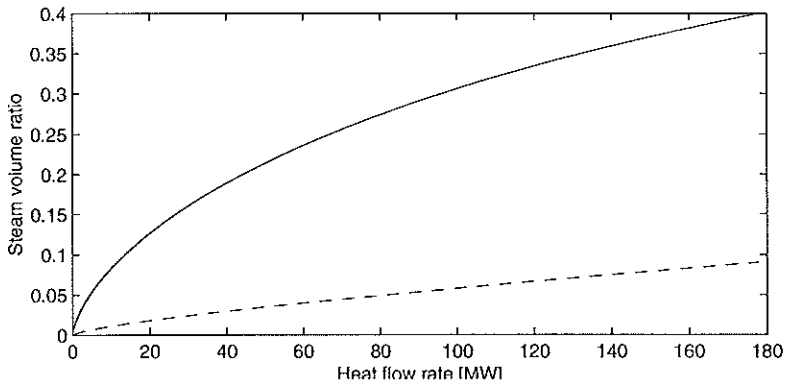

Figure 3 Steady state relation between steam volume ratio $\bar{\alpha}_v$ and input power Q. The dashed curve shows the steam mass ratio α_r.

Equilibrium Values

The steady state solution of Equation (26) is given by

$$\begin{aligned} q_f &= q_s \\ Q &= q_s h_s - q_f h_f \\ Q &= q_{dc} \alpha_r h_c \\ V_{sd} &= V_{sd}^0 - \frac{T_d(h_w - h_f)}{\rho_s h_c} q_f. \end{aligned}$$

where q_{dc} is given by Equation (16), i.e.

$$q_{dc} = \sqrt{\frac{2\rho_w A_{dc}(\rho_w - \rho_s) g \bar{\alpha}_r V_r}{k}}.$$

A convenient way to find the initial values is to first specify steam flow rate q_s and steam pressure p. The feedwater flow rate q_f and the input power Q are then given by the first two equations and the steam volume in the drum is given by the last equation. The steam quality α_r is obtained by solving the equations

$$\begin{aligned} Q &= \alpha_r h_c \sqrt{\frac{2\rho_w(\rho_w - \rho_s) g \bar{\alpha}_v V_r}{k}} \\ \bar{\alpha}_v &= \frac{\rho_w}{\rho_w - \rho_s}\left(1 - \frac{\rho_s}{(\rho_w - \rho_s)\alpha_r} \ell n\left(1 + \frac{\rho_w - \rho_s}{\rho_s}\alpha_r\right)\right). \end{aligned} \tag{29}$$

The steam volume in the drum can then be computed directly.

Equation (29) defines the steam volume ratio $\bar{\alpha}_v$ as a function of the input power Q. This function which is shown in Figure 3 gives important insight into the shrink and swell phenomena. The curve shows that a given change in input power gives a larger variation in average steam volume ratio at low power. This explains why the shrink and swell effects are larger at low power than at high power. The derivative of the function $\bar{\alpha}_v = f(Q)$ changes with about a factor of 5 in the range shown in Figure 3.

Matlab Code

Appendix B gives the model in the format of an S-function for Simulink. This code was used to run all simulations in the paper, particularly all the curves in Sections 5 and 6 were generated in this way. The code is based on Equation (26) which can be written as

$$E\frac{dx}{dt} = b.$$

The elements of the matrix E are given by Equation (27). The matrix E and the vector b are first computed and the derivative of the state is obtained using Matlab's matrix inversion. The variable names used and the structure of the code has been kept as close as possible to the notation in the paper. Quadratic approximations of the steam tables are also given in the code.

Impact of Modeling Languages

Development of physical models is a tedious iterative process. Different physical assumptions are made, a model is developed and compared with experiments by simulation, parameters may be fitted. Detailed investigation of the results gives ideas for improvements and modifications. It is a significant effort to transform the equations to state space form because of the algebra involved. This is reflected in the manipulations resulting in Equation (27). Many intermediate steps have actually been omitted in the paper. The modeling effort can be reduced substantially by using modeling languages such as Dymola, [22], Omola, [38], or Modelica, [23]. In these languages the model is described in it most basic form in terms of differential algebraic equations. In our case this means that the basic mass and energy balances, such as (1) and (2), are entered into the system together with the algebraic equations, such as (5). The software then makes algebraic manipulations to simplify the equations for efficient simulation. Preliminary experiments indicate that the effort required to develop the model described in this paper can be reduced by a factor of 5. The ease of evaluating many alternatives also makes it possible to try many different hypotheses.

5. Step Responses

To give some insight into the properties of the model we will present some step responses. Since there are many inputs and many interesting variables we will focus on a few selected responses. One input was changed and the others were kept constant. The magnitudes of the changes were about 10% of the nominal values of the signals. To compare responses at different load conditions the same amplitudes were used at high and medium load. The drum level was normalized to zero by altering the total amount of water in the system. This corresponds to the situation that normally occurs in operation with level control.

Plant Parameters

To illustrate the dynamic behavior of the model we will simulate responses to step changes in the inputs. These were generated from a simulation

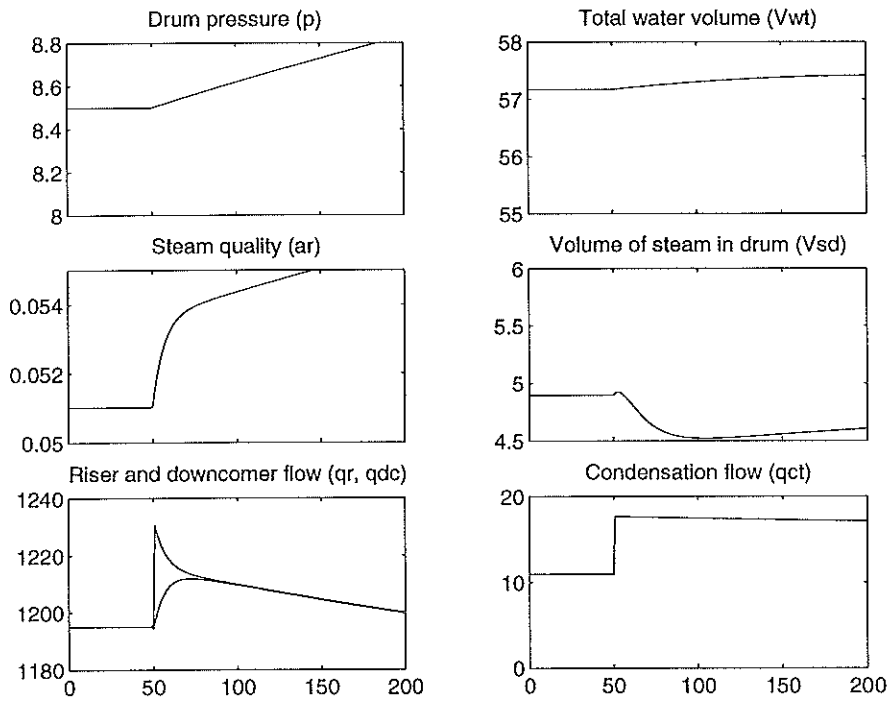

Figure 4 Responses to a step corresponding to 10 MW in fuel flow rate at medium load.

of the model. The parameters used were those from the Swedish power plant. The values are $V_d = 40m^3$, $V_r = 37m^3$, $V_{dc} = 11m^3$, $A_d = 20m^2$, $m_t = 300000kg$, $m_r = 160000kg$, $k = 25$, $\beta = 0.3$ and $T_d = 12s$. The quadratic approximations of the steam tables given in the computer code in Appendix B were used in the simulations.

Fuel Flow Changes at Medium Load

Figure 4 shows the responses of the state variables, the circulation flow rate q_{dc}, the riser flow rate q_r and the total condensation flow q_{ct} to a step increase in fuel flow rate equivalent to 10 MW.

Pressure increases at approximately constant rate. The reason for this is that steam flow out of the drum is constant. Total water volume V_{wt} increases due to the condensation that occurs due to the increasing pressure. Steam quality at the riser outlet α_r first increases rapidly and then more gradually. The volume of steam in the drum first increases a little and it then decreases. The rapid initial increase in steam volume is due to the fast increase in steam from the risers. The decrease is due to the increased pressure which causes condensation of the steam. At the onset of the step there is a rapid increase in the outlet flow rate from the risers. The flow then decreases to match the downcomer flow rate. The flow rates are equal after about 30 seconds. The condensation flow changes in an almost step like manner.

Steam Flow Changes at Medium Load

Figure 5 shows the responses to a step increase of 10 kg/s in steam flow at medium load. Pressure decreases practically linearly because of the in-

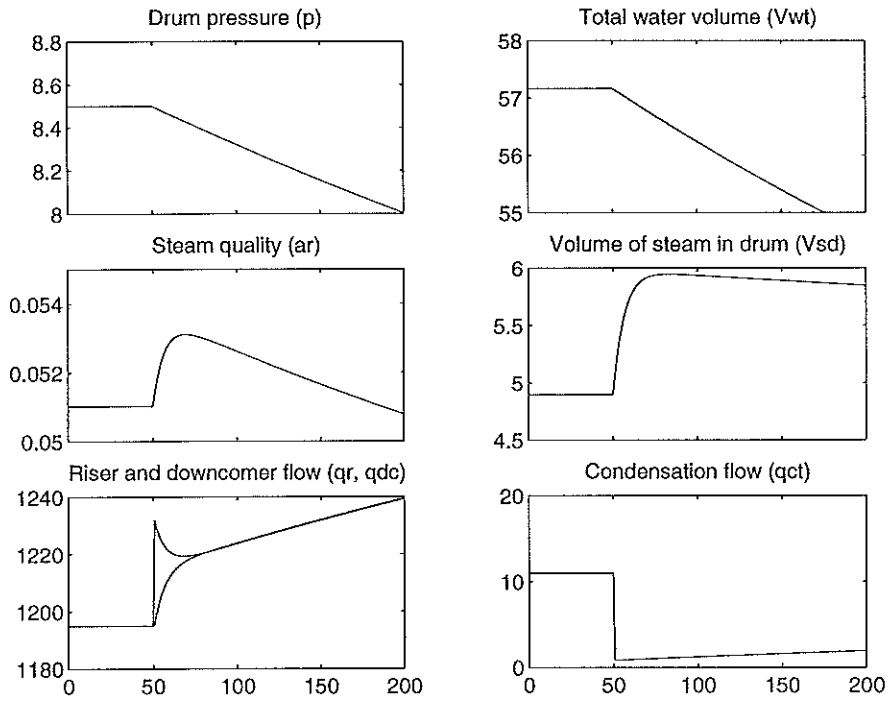

Figure 5 Responses to a step of 10 kg/s in steam flow rate at medium load.

creased steam flow. Total water volume also decreases because of increased evaporation due to the decreasing pressure. Steam quality at the riser outlet first increases rapidly due to the pressure decrease and it then decreases due to the increased circulation flow rate. The volume of the steam in the drum increases due to the decreased pressure. There is a very rapid increase of flow out of the riser due to the pressure drop. After this initial transient the riser flow rate then decreases to match the downcomer flow rate. There is a steady increase in both due to the decreased pressure. The condensation flow drops in an almost step like fashion because the pressure decreases at constant rate.

Drum Level Responses

Since the behavior of the drum level is of particular interest we will show step responses that give good insight into drum level dynamics for different operating conditions. It follows from Equation (22) that drum level is the sum of $\ell_w = V_{wd}/A_d$ and $\ell_s = V_{sd}/A_d$, which depend on the volumes of water and steam in the drum. Drum pressure, steam mass and volume fractions will also be shown. Responses for medium and high load will be given to illustrate the dependence on oerating conditions.

Figure 6 shows the response to a step in fuel flow corresponding to 10 MW. The response in drum level is complicated and depends on a combination of the dynamics of water and steam in the drum. The initial part of the swell is due to the rapid initial response of steam that was also seen in Figure 4. The response in level is a combination of two competing mechanisms. The water volume in the drum increases due to increased condensation caused by the increasing pressure. The volume of the steam in the drum first increases a little and it then decreases because of the increasing

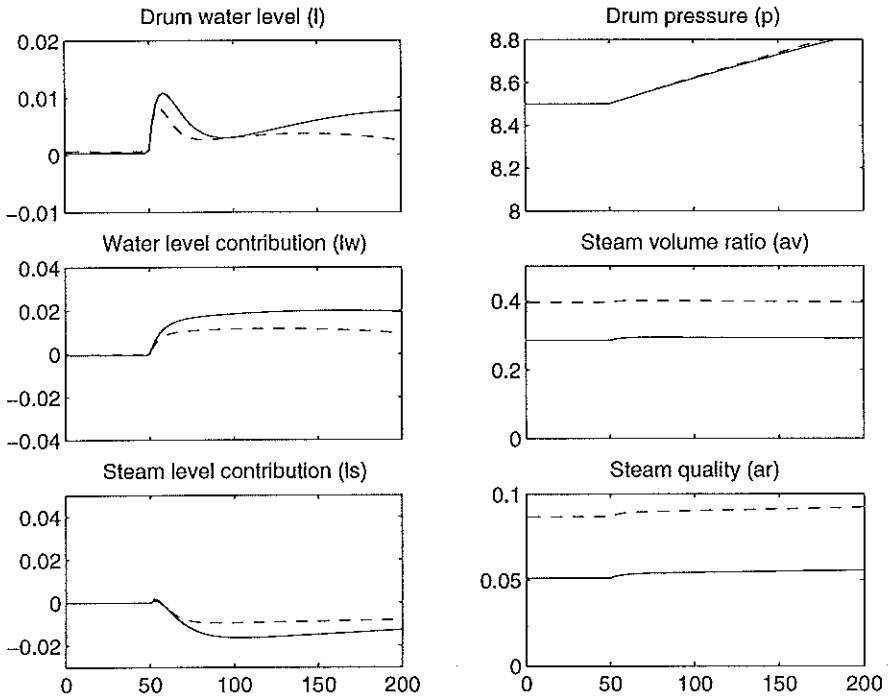

Figure 6 Responses to a step change corresponding to 10 MW in fuel flow rate at medium (solid) and high (dashed) loads.

pressure. Notice that there are significant changes in steam quality and steam volume ratio for the different operating conditions. Compare with Figure 3.

Figure 7 shows the response to a step increase in steam flow rate of 10 kg/s. There is a strong shrink and swell effect in this case too. The contributions from the volumes of steam and water have initially the same sign. The water volume will, however, decrease because of the steam flow.

Figure 8 shows the response to a step increas in feedwater flow rate of 10 kg/s. The shrink and swell effect is clearly visible. Notice that the non-minimum phase nature of the response is much larger at medium load. A rough estimate of the zero in the right half plane shows that the zero is approximately 4 times slower at medium load. This indicates that it is more difficult to control the system at medium load. In this case the water and the steam in the drum also respond in opposite directions. The water level increases because of the increasing water and the steam level decreases because of the condensation required to heat the feedwater.

Figure 9 shows the response to a step increase in feedwater temperature of 10°C. In this case the response is dominated by the dynamics of the volume of the steam in the drum. The contribution of the water in the drum is an order of magnitude smaller.

In summary we find that the shrink and swell effect is clearly noticeable in all responses. The dynamics of the drum level is influenced by the dynamics of steam and water in the drum. In some situations steam and water reacts in the same way to changes in the input but in other cases they react in opposite ways. This results in a complex behavior. The response to fuel flow changes is the most complicated response because this

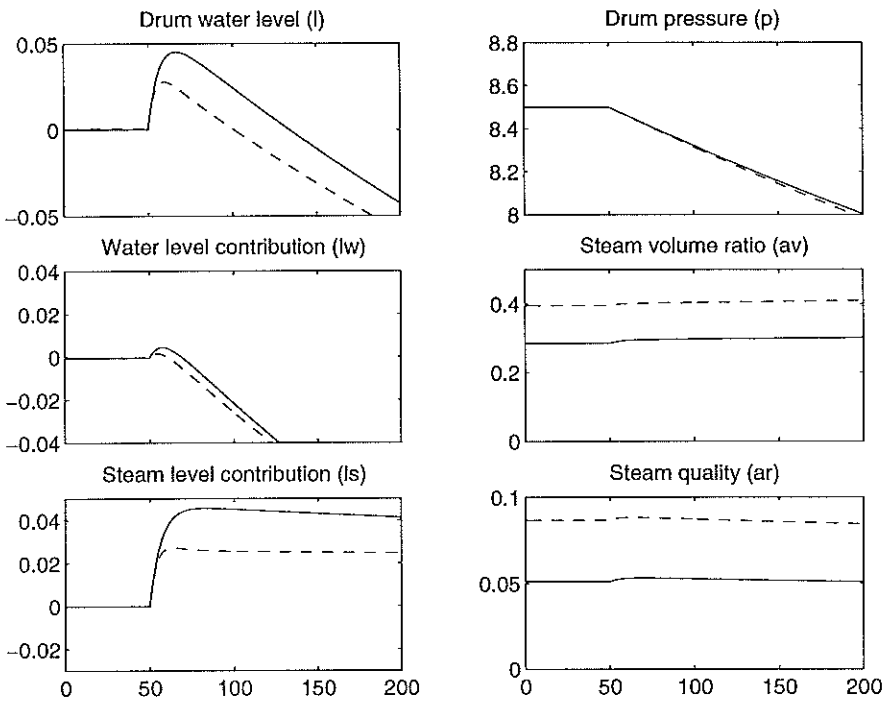

Figure 7 Responses to a step change of 10 kg/s in steam flow rate at medium (solid) and high (dashed) loads.

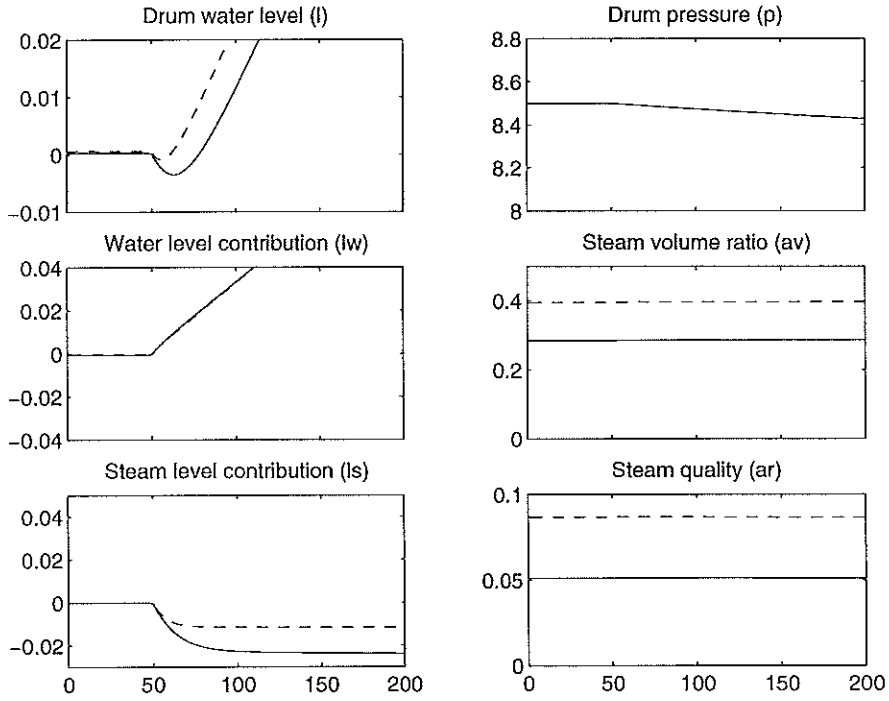

Figure 8 Responses to a step change of 10 kg/s in feedwater flow rate at medium (solid) and high (dashed) loads.

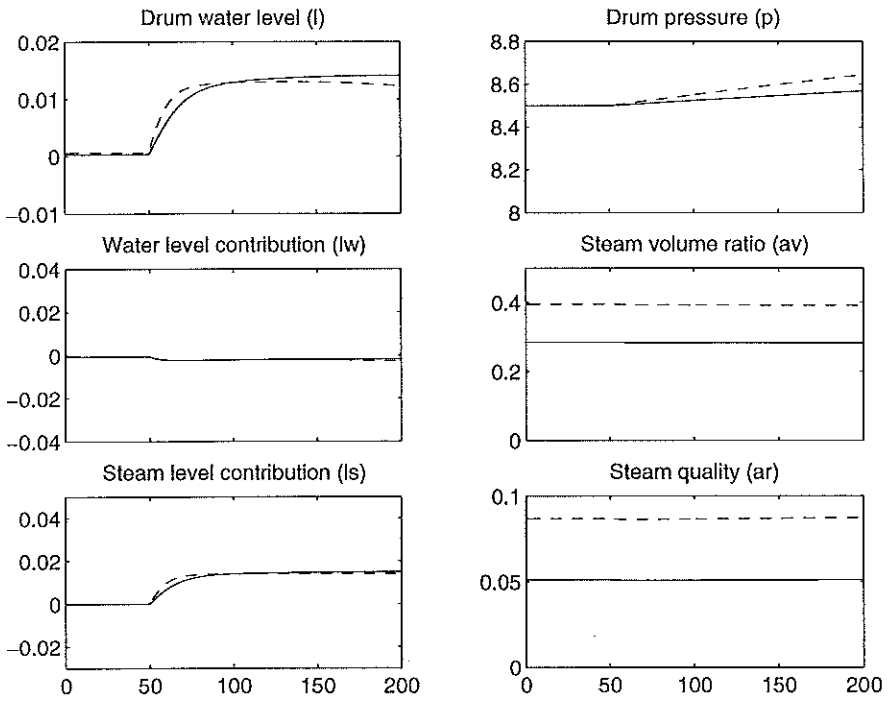

Figure 9 Responses to a step change of 10° C in feedwater temperature at medium (solid) and high (dashed) loads.

perturbation excites the drum and the riser in different ways. The shrink and swell effect is larger at lower power levels. This follows from the discussion of Figure 3.

6. Comparisons with Plant Data

Much of the model development was based on plant experiments performed with the P16-G16 unit at Öresundsverket in Malmö, Sweden in collaboration with Sydkraft AB. The experiments are described in [21], [7], and [8]. They were carried out in open loop with the normal regulators removed. The signals were filtered and sampled at a rate of 0.1 Hz. To ensure a good excitation of the process PRBS-like perturbations were introduced in fuel flow rate, feedwater flow rate and steam flow rate. The intention was to change one input signal in each experiment. To ensure that critical variables such as drum water level did not go outside safe limit we made manual correction occasionally. This means that several inputs were changed in each experiment. The steam flow rate changed in response to pressure changes in all experiments because we were unable to control it tightly.

A large number of signals were logged during the experiment. This proved to be very valuable because it has been possible to use the data for a very large number of investigations. The experiments were performed both at high and medium load. In this paper we have used data where three variables, fuel flow rate, feedwater flow rate, and steam flow rate were changed. This gives a total of 6 experiments which can be used to

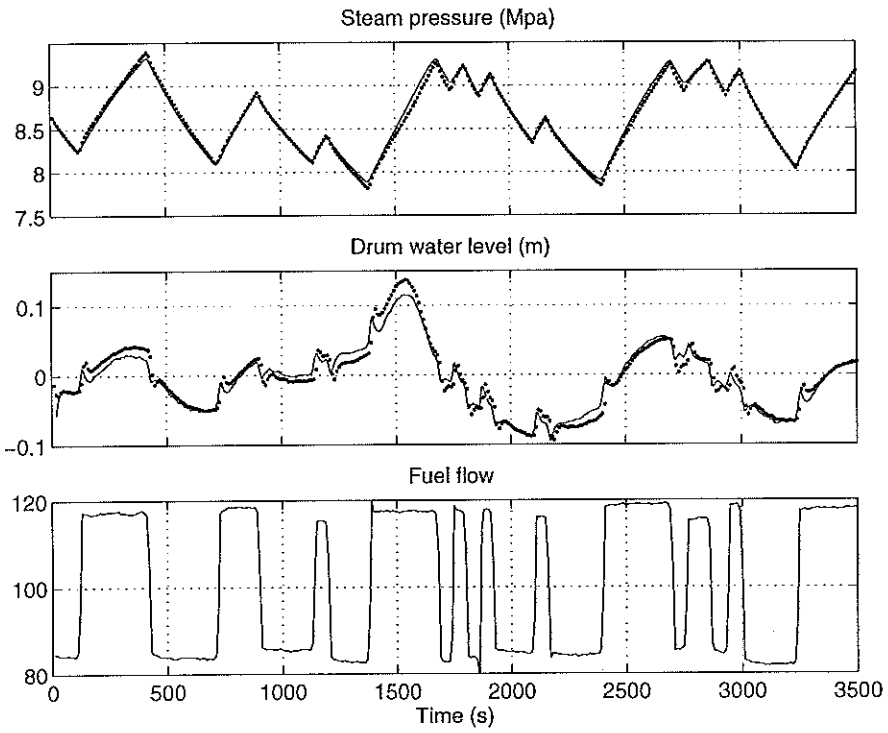

Figure 10 Comparison of model (solid line) and plant data (dots) for perturbations in fuel flow rate at medium load.

validate the model.

There were problems with the calibration of the flow rate measurement transducers and also some uncertainty in the effective energy content of the oil. The approach used was to start with the nominal calibration values and then make small corrections so that the long term tracking between the plant data and the model was as close as possible. The change in all cases was well within the transducers accuracy limits. Apart from that, no fiddling with the coefficients was made. When showing the results in the following, we present the primary input variable and the responses in drum pressure and drum level.

Experiments at Medium Load

The results of experiments at medium load will be described first. This is the operating condition where the shrink and swell phenomenon is most pronounced.

Fuel Flow Rate Changes Figure 10 shows responses in drum pressure and drum level for perturbations in fuel flow rate. There is very good agreement between the model and the experimental data for drum pressure and drum water level. Notice in particular that there is an overshoot in the drum level response for step changes in fuel flow. We call this phenomenon the rapid swell. We have not found any previous references to this phenomenon. It is due to interaction between the two state variables that describe the dynamics of steam under the liquid level in the drum.

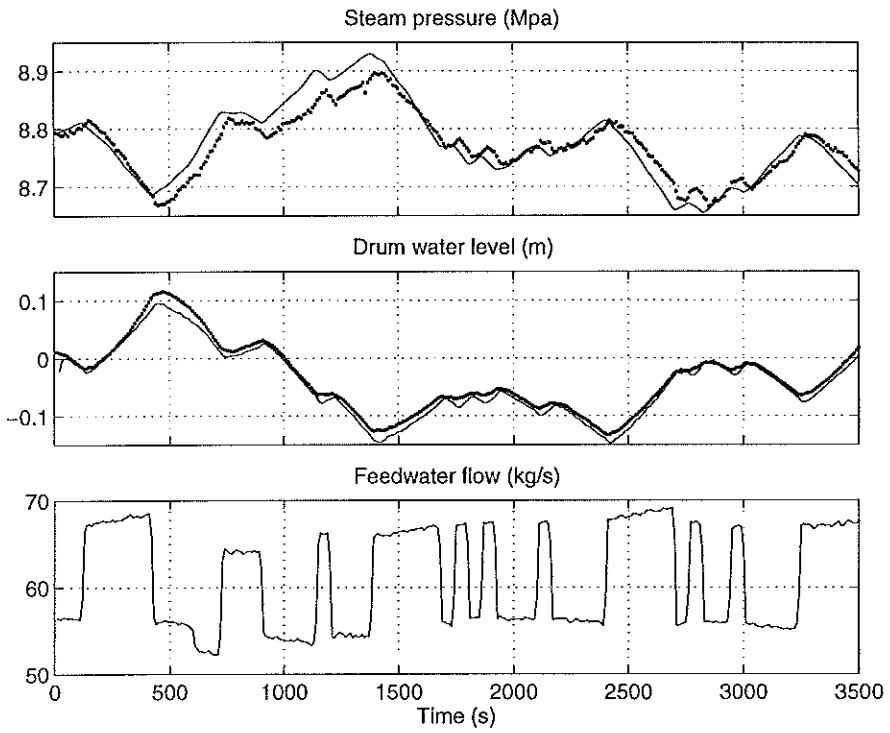

Figure 11 Comparison of model (solid line) and plant data (dots) for perturbations in feedwater flow rate at medium load.

Changes in Feedwater Flow Rate Figure 11 shows the responses to changes in the feedwater flow rate. The general character of the responses agree well there are some deviations in the pressure responses and some of the finer details of the drum level are exaggerated. The pressure does deviate in the 500 to 1500 second region, but since the changes in pressure are small the results are considered adequate.

Changes in the Steam Valve Figure 12 shows the responses to changes in the steam valve. There is very good agreement between the model and the experimental data. Notice that there is a significant shrink swell effect which is captured very well by the model.

Experiment at High Load

Changes in Fuel Flow Rate Figure 13 shows responses in drum pressure and drum level for perturbations in fuel flow rate. There is good agreement between the model and the experimental data. A comparison with Figure 10 shows that the shrink and swell effect is much smaller at high load. It is interesting to see that the model captures this.

Changes in Feedwater Flow Rate Figure 14 shows the responses to changes in feedwater flow rate. There are discrepancies in pressure from time 400 to 1400. The total changes in pressure are small and minor variations in feedwater conditions can easily cause variations of this magnitude. The model exaggerates the level changes for rapid variations. Compare for example data in the interval 1500 to 2000.

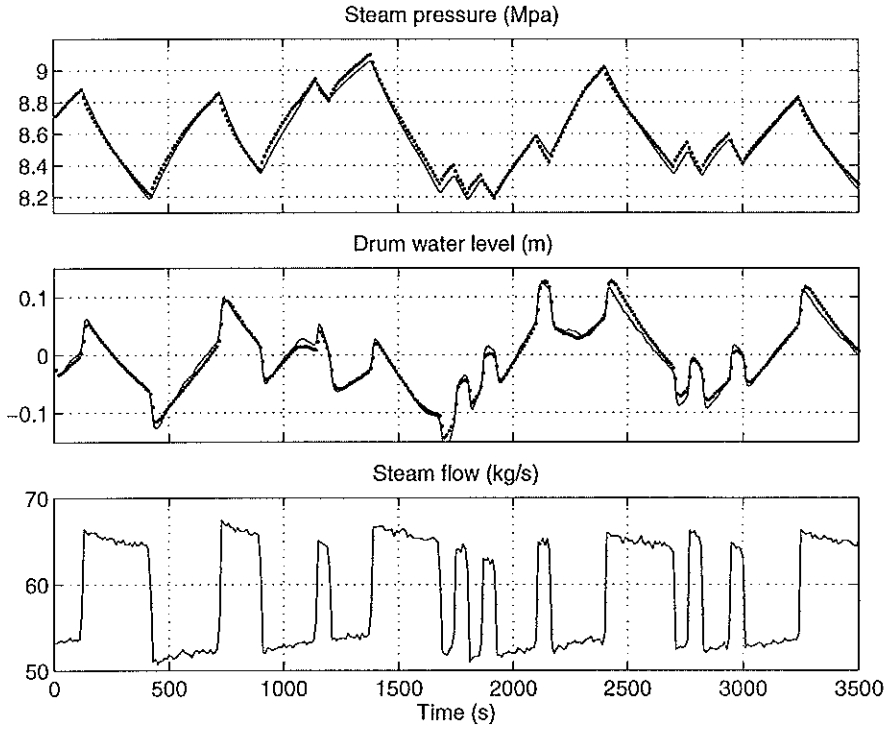

Figure 12 Comparison of model (solid line) and plant data (dots) for perturbations in steam flow rate at medium load.

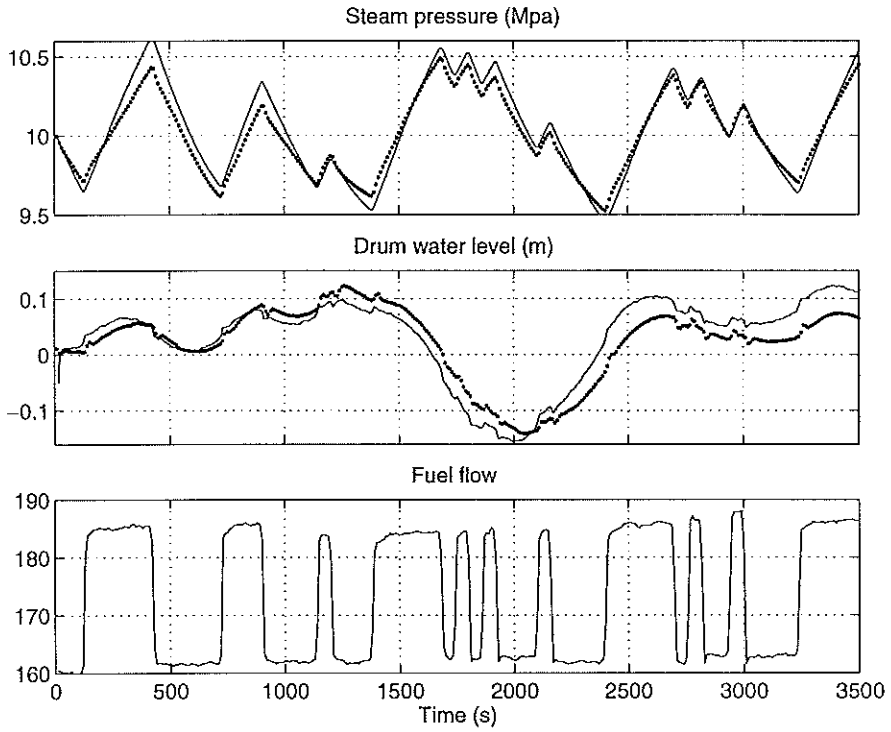

Figure 13 Comparison of model (solid line) and plant data (dots) for perturbations in fuel flow rate at high load.

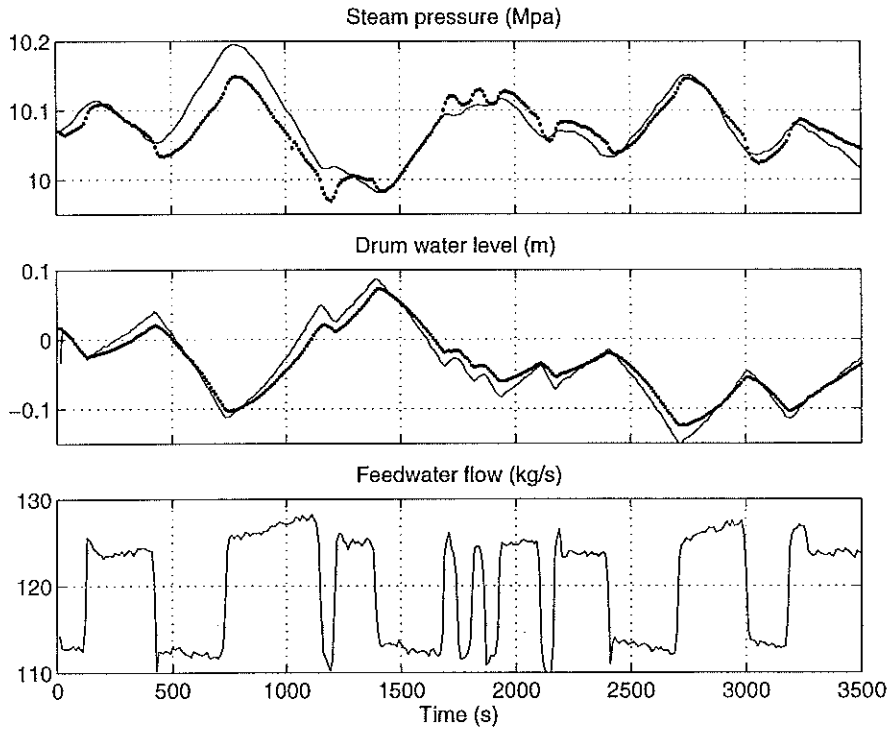

Figure 14 Comparison of model (solid line) and plant data (dots) for perturbations in feedwater flow rate at high load.

Changes in the Steam Valve Figure 15 shows the responses to changes in the steam flow rate. There is very good agreement between the model and the experimental data. Notice that the model captures the drum level variations particularly the swell and shrink effect very well. A comparison with Figure 12 shows that the shrink and swell effect is smaller at high loads. This is well captured by the model.

Comparison of Behavior at High and medium Load

The experiments have indicated that there are significant differences in behavior at high and medium loads that are well predicted by the model. We will now look closer at these differences.

Figure 16 compares the responses in drum level to steam flow changes at high and medium loads. The steam valve changes were almost the same in both experiments (as is shown in Figures 12 and 15) but they were not identical. Figure 16 shows that the model matches the experiments very well and it also shows that the shrink and swell effect is larger at medium load. Figure 17 compares responses to changes in fuel flow. Notice the good agreement between model and experiments. In this case there is a pronounced difference between the behaviors for medium and high load. Figure 18 also compares responses to changes in fuel flow. We have taken a section of the data where there are substantial rapid variations. Again we notice the excellent agreement between model and experiments and we also notice the significant difference between the behaviors at medium and high loads.

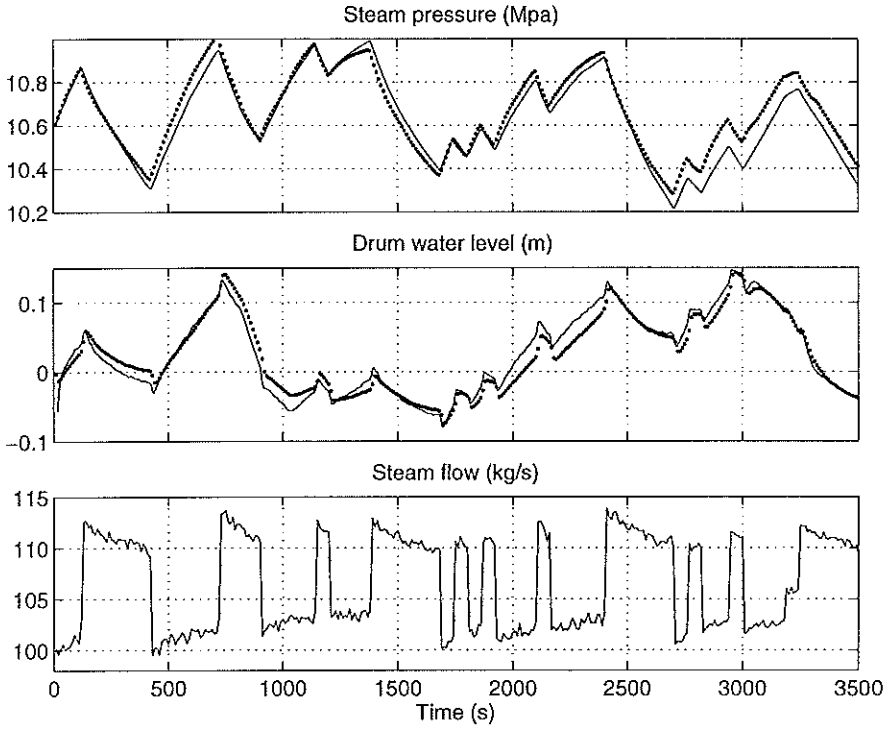

Figure 15 Comparison of model (solid line) and plant data (dots) for perturbations in steam flow rate at high load.

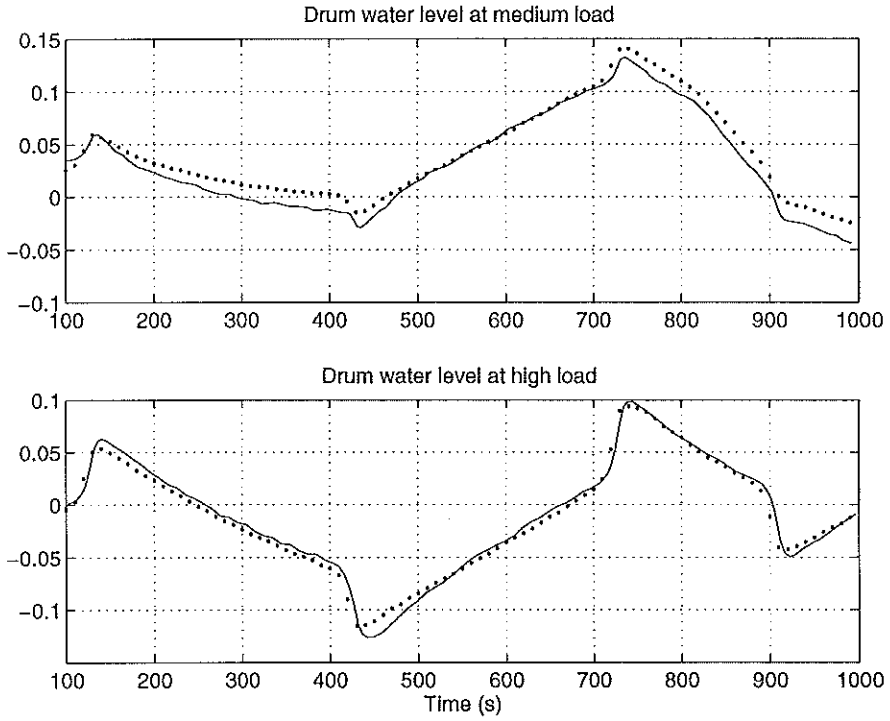

Figure 16 Comparison of behavior of drum water level at medium and high loads for perturbations in steam flow rate. The model response is shown in solid lines and plant data is indicated by dots.

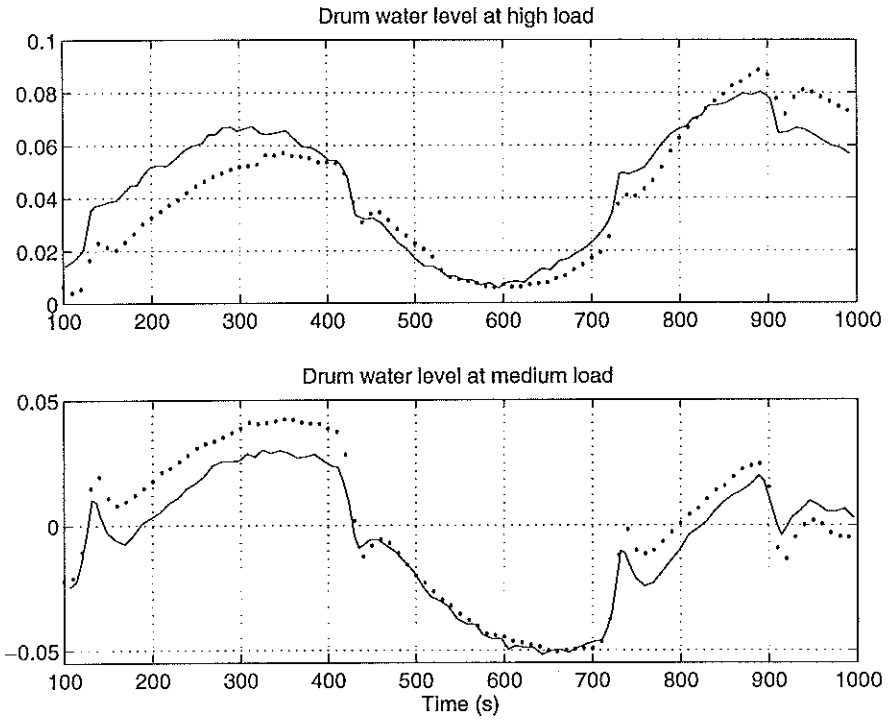

Figure 17 Comparison of behavior of drum water level at medium and high loads for perturbations in fuel flow rate. The model response is shown in solid lines and plant data is indicated by dots.

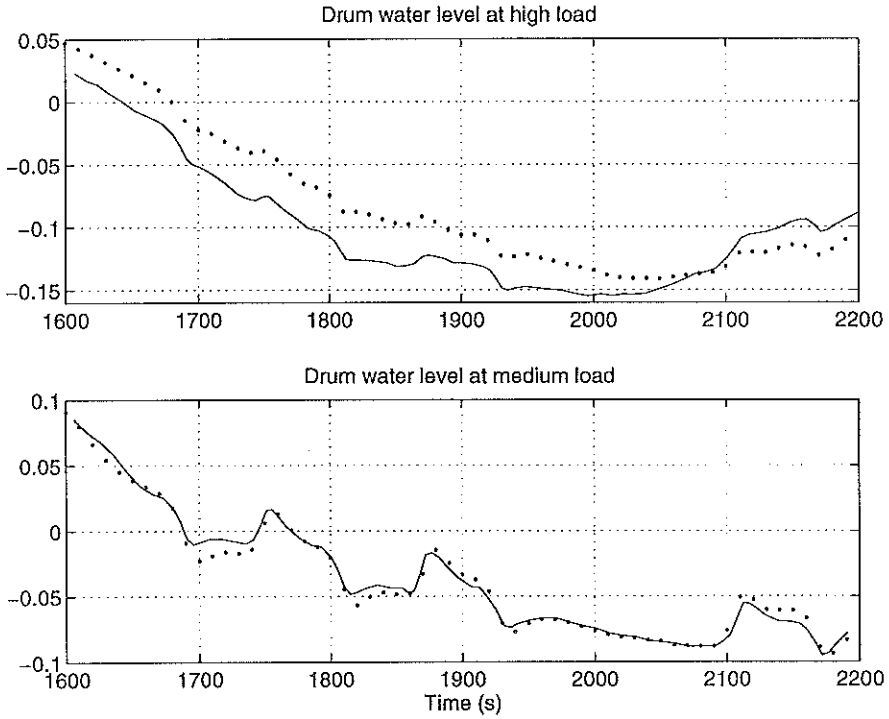

Figure 18 Comparison of behavior of drum water level at medium and high loads for perturbations in fuel flow rate. The model response is shown in solid lines and plant data is indicated by dots.

7. Conclusions

A nonlinear physical model with a complexity that is suitable for model based control has been presented. The model is based on physical parameters for the plant and can be easily scaled to represent any drum power station. The model has four states; two account for storage of total energy and total mass, one characterizes steam distribution in the risers and another the steam distribution in the drum. The model can be characterized by a few physical parameters and steam tables.

The model is nonlinear and agrees well with experimental data. In particular, the complex shrink and swell phenomena associated with the drum water level are well captured by the model. The model has a triangular structure that can be described as $(((V_{wt}, p), \alpha_r), V_{sd})$, where the states in each bracket can be determined sequentially. The linearized model has two poles at the origin and two real stable poles.

The model has been validated against plant data with very rich excitation that covers a wide operating range. These experiments have given much insight into the behavior of the system and it has guided the modeling effort. We believe that the approach used in this work can be applied to other configurations of steam generators.

The model (26) can be simplified by keeping only the dominant terms in the expressions (27) for the coefficients e_{ij}. This could be useful for applications to model based control. Preliminary experiments indicate that several terms can be neglected without sacrificing the fit to experimental data. A comprehensive study of this is outside the scope of this paper. The model can also be refined. One possibility is to introduce dynamics in the momentum equations for circulation flow. This could be useful in order to give a more detailed description of the phenomenon we called rapid swell. Our experimental data did not allow this because the sampling rate was 10s.

Acknowledgments

We would like to express our sincere gratitude to Sydkraft AB for financial support, discussions with staff and particularly for their willingness to perform experiments on plants to increase our understanding of the plant's behavior.

8. References

[1] N. N. AMPOS, N. N. DUC, and N. N. FALIOWER. "Application of $\mathcal{H}_2$ control design with disturbance feedforward in steam generator level in edf pwr units." In *Proc. CESA'96 IMACS*, pp. 1299–1304, 1996.

[2] P. M. ANDERSON. *Modeling Thermal Power Plants for Dynamic Stability Studies.* Book Cyclone Copy Center, Ames, Iowa, 1974.

[3] P. M. ANDERSON and S. NANAKORN. "An analysis and comparison of certain low-order boiler models." *ISA 1974*, 1974.

[4] K. J. ÅSTRÖM. "Modelling and identification of power system components." In HANDSCHIN, Ed., *Real-time Control of Electric Power Sys-*

tems, Proc. Symp. on Real-time Control of Electric Power System, Baden, Switzerland, 1971, pp. 1–28. Elsevier, 1972.

[5] K. J. ÅSTRÖM and R. BELL. "Simple drum-boiler models." In *IFAC Int. Symposium on Power Systems, Modelling and Control Applications*, Brussels, Belgium, 1988.

[6] K. J. ÅSTRÖM and R. D. BELL. "A nonlinear model for steam generation process." In *Preprints IFAC 12th World Congress*, Sydney, Australia, July 1993.

[7] K. J. ÅSTRÖM and K. EKLUND. "A simplified non-linear model for a drum boiler—Turbine unit." *International Journal of Control*, **16**, pp. 145–169, 1972.

[8] K. J. ÅSTRÖM and K. EKLUND. "A simple non-linear drum-boiler model." *International Journal of Control*, **22**, pp. 739–740, 1975.

[9] R. D. BELL. *The on-line optimal control of constrained non-linear processes and its application to steam generators*. PhD thesis, University of N.S.W., Australia, March 1973.

[10] R. D. BELL and K. J. ÅSTRÖM. "A fourth order non-linear model for drum-boiler dynamics." In *IFAC'96, Preprints 13th World Congress of IFAC*, vol. O, pp. 31–36, San Francisco, California, July 1996.

[11] R. D. BELL, N. W. REES, and K. B. LEE. "Models of large boiler-turbine plant." In *IFAC Symposium on Automatic Control & Protection of Electric Power Systems*, pp. 469–475. Ins. of Engineers, Aust. National Conf. Publ., 1977.

[12] T. BOHLIN. *Interactive System Identification: Prospects and Pitfalls*. Springer-Verlag, 1991.

[13] L. BORSI. "Extended linear mathematical model of a power station unit with a once through boiler." *Siemens Forschungs und Entwicklingsberichte*, **3:5**, pp. 274–280, 1974.

[14] P. CASEAU and P. GODIN. *Mathematical modelling of power plants*. IE(Aust) Elect. Eng. Trans., March 1969.

[15] C. CHENG and N. REES. "Fuzzy model based control of steam generation in drum-boiler power plant." In *Proc. IFAC/CIGRE Symposium on Control of Power Systems and Power Plants CPSPP'97, Beijing, China*, pp. 175–181. International Academic Publishers, 1997.

[16] K. L. CHIEN, E. I. ERGIN, C. LING, and A. LEE. "Dynamic analysis of a boiler." *Trans. ASME*, **80**, pp. 1809–1819, 1958.

[17] F. P. DE MELLO. "Plant dynamics and control analysis." In *IEEE Transactions on Power Apparatus and Systems*, vol. S82, pp. 664–678, 1963. Paper 63-1401.

[18] M. DENN, MOTRON. *Process Modelling*. Wiley, New York, 1987.

[19] R. DOLEZAL and L. VARCOP. *Process dynamics*. Elsevier Publ. Co., 1970.

[20] J. EBORN and J. SØRLIE. "Parameter optimization of a non-linear boiler model." In SYDOW, Ed., *15th IMACS World Congress*, vol. 5, pp. 725–730, Berlin, Germany, August 1997. W & T Verlag.

[21] K. EKLUND. *Linear Drum Boiler-Turbine Models.* PhD thesis TFRT-1001, Department of Automatic Control, Lund Institute of Technology, Lund, Sweden, November 1971.

[22] H. ELMQVIST. *A Structured Model Language for Large Continuous Systems.* PhD thesis TFRT-1015, Department of Automatic Control, Lund Institute of Technology, Lund, Sweden, May 1978.

[23] H. ELMQVIST, S. E. MATTSSON, and M. OTTER. "Modelica — The new object-oriented modeling language." In *Proceedings of the 12th European Simulation Multiconference (ESM'98)*, Manchester, UK, 1998. SCS, The Society for Computer Simulation.

[24] C. E. GARCIA, D. M. PRETT, and M. MORARI. "Model predictive control: Theory and practice - A survey." *Automatica*, **25:3**, pp. 335–348, 1989.

[25] E. HAIRER, C. LUBICH, and M. ROCHE. *The Numerical Solution of Differential-Algebraic Systems by Runge-Kutta Methods.* Lecture Notes in Mathematics No. 1409. Springer-Verlag, Berlin, 1989.

[26] P. A. HEUSSER. *Modelling and simulation of boiling channels with a general front tracking approach.* Society for ComputerSimulation, Inc, San Diego, 1996.

[27] A. HÖLD. "Utsg-2 - a theoretical model describing the transient behavior of a pressurized water reactor natural-circulation u-tube steam generator." *Nuclear Technology*, **90**, pp. 98–118, 1990.

[28] J. JARKOVSKY, J. FESSL, and V. MEDULOVA. "A steam generator dynamic mathematical modelling and its using for adaptive control systems testing." In *Preprints IFAC Symposium on Power Systems Modelling and Control Applications*, Brussels, Belgium, 1988.

[29] G. KLEFENZ. *Automatic Control of Steam Power Plants.* Bibliographisches Institut, third edition, 1986.

[30] S. S. KUTATELADZE. "Heat transfer in condensation and boiling." Technical Report AEC-tr-3770, United States Atomic Energy Commission, August 1959.

[31] H. W. KWAN and J. H. ANDERSSON. "A mathematical model of a 200 MW boiler." *Int. Journal of Control*, **12**, pp. 977–998, 1970.

[32] H. G. KWATNY and J. BERG. "Drum level regulation at all loads." In *Preprints IFAC 12th World Congress*, vol. 3, pp. 405–408, Sydney, Australia, 1993.

[33] S. LINDAHL. *Design and Simulation of a Coordinated Drum Boiler-Turbine Controller.* Lic Tech thesis TFRT-3143, Department of Automatic Control, Lund Institute of Technology, Lund, Sweden, December 1976.

[34] C. X. LU, R. BELL, and N. REES. "Scheduling control of deaerator plant." In *Proc. IFAC/CIGRE Symposium on Control of Power Systems and Power Plants CPSPP'97, Beijing, China*, pp. 219–226. International Academic Publishers, 1997.

[35] C. MAFFEZZONI. *Dinamica dei generatori di vapore.* Hartman and Braun, Milano, 1988.

[36] C. MAFFEZZONI. "Issues in modeling and simulation of power plants." In *Proc. IFAC Symp. Control of Power Plants and Power Systems*, vol. 1, pp. 19–27, 1992.

[37] C. MAFFEZZONI. "Boiler-turbine dynamics in power plant control." In *IFAC 13th Triennial World Congress*, San Francisco, USA, 1996.

[38] S. E. MATTSSON, M. ANDERSSON, and K. J. ÅSTRÖM. "Object-oriented modelling and simulation." In LINKENS, Ed., *CAD for Control Systems*, pp. 31–69. Marcel Dekker, Inc, 1993.

[39] D. Q. MAYNE, J. B.RAWLINGS, and C. V. RAO. "Model predictive control: A review." *Automatica*, p. To appear, 1999.

[40] J. P. MCDONALD, G. H. KWATNY, and J. H. SPARE. "A nonlinear model for reheat boiler-turbine generation systems." *Proceedings JACC*, pp. 227–236, 1971.

[41] J. P. MCDONALD and H. G. KWATNY. "A mathematical model for reheat boiler-turbine-generator systems." In *Proc. IEEE*, New York, 25-30 January 1970. PES Winter Power Meeting. Paper 70 CP221-PWR.

[42] N. MILLER, J. BENTSMAN, D. DRAKE, J. FAKHFAKH, T. JOLLY, G. PELLEGRINETTI, and J. TSE. "Control of steam generation processes." In *Proc. ISA 90*, pp. 1265–1279, New Orleans Lousiana, 1990.

[43] A. J. MORTON and P. H. PRICE. "The controllability of steam output, pressure and water level in drum boilers." *Proc. I. Mech. Eng.*, pp. 75–84, 1977.

[44] H. NICHOLSON. "Dynamic optimisation of a boiler." In *Proc. IEE*, vol. 111, pp. 1479–1499, August 1964.

[45] A. PARRY, J. F. PETETROT, and M. J. VIVIER. "Recent progress in sg level control in french pwr plants." In *Proc. Int. Conf on Boiler Dynamics and Control in Nuclear Powerstations*, pp. 81–88. British Nuclear Energy Society, 1995.

[46] G. PELLEGRINETTI, J. BENTSMAN, and K. POLLA. "Control of nonlinear steam generation processes using h^∞ design." In *Proc. 1991 ACC Boston, MA*, pp. 1292–1297, 1991.

[47] P. PROFOS. "Dynamics of pressure and combustion control in steam generators." *Sulzer Technical Review*, **4**, pp. 1–15, 1955. V37.

[48] P. PROFOS. *Die Regelung von Dampfanlagen*. Springer-Verlag, Berlin, 1962.

[49] S. QIN and T. A. BADGWELL. *An overview of industrial model predictive control technology*, vol. 97. AIChE Symposium Series, 1997.

[50] G. QUAZZA. "Sui modelli analitici delle caldaie a corpo cilindrico. Parte I: Dinamica del vaporizzatore." *Automazione e Strumentazione*, pp. 506–537, 1968.

[51] G. QUAZZA. "Automatic control in electric power systems." *Automatica*, **6**, pp. 123–150, 1970.

[52] J. SØRLIE and J. EBORN. "A Grey-box Identification Case Study: The Åström–Bell Drum-boiler Model." Technical Report, Department of Automatic Control, Lund Institute of Technology, Lund, Sweden, To appear 1998.

[53] C. B. SPEEDY, R. D. BELL, and G. C. GOODWIN. "Dynamic modelling of a steam generator using least squares analysis." *JACC*, 1970.

[54] F. T. THOMPSON. *A dynamic model for control of a drum type boiler system.* PhD thesis, University of Pittsburg, USA, 1964.

[55] A. TYSSØ, J. C. BREMBO, and K. LIND. "The design of multivariable control system for a ship boiler." *Automatica*, **12**, pp. 211–224, 1976.

[56] H. UNBEHAUEN and I. KOCAARSLAN. "Experimental modelling and adaptive power control of a 750 MV once-through boiler." In *Preprints IFAC 11th World Congress on Automatic Control*, vol. 11, pp. 32–37, Tallinn, Estonia, 1990.

[57] R. C. WALTERS and T. J. WILLIAMS. "A linearised mathematical model for the dynamics and control of the propulsion system (steam boiler-turbine) of a naval vessel." In *IFAC Symposium in Sidney*, August 1969. Paper No. 2570.

[58] M. R. YEUNG and P. L. CHAN. "Development and validation of a steam generator simulation model." *Nuclear Technology*, **92**, pp. 309–314, 1990.

Appendix A - Plant Parameters

```
% The physical constants for the two plants
% Australian Plant
        Ad= 52;
        Vd= 73;
        mt=2000000;
        Vr= 36;
        Vdc= 60;
        ke=200;
        Cp=650;

% Swedish Plant
        Ad= 23;
        Vdrum= 37;
        mt=300000;
        mr=100000;
        Vr= 37;
        Vdc= 11;
        k=200;
        Cp=650;
        beta=0.3;

% Coefficients for quadratic fit to steam tables.
% Properties of steam and water in saturated state.
        a01= 2.7254E6;
        a11= -1.8992E4;
        a21= -1160.0;

        a02= 53.1402;
        a12= 7.673;
        a22= 0.36;

        a03= 1.4035E6;
        a13= 4.9339E4;
        a23= -880.0;

        a04= 691.35;
        a14= -18.672;
        a24= -0.0603;

        a05= 310.6;
        a15= 8.523;
        a25= -0.33;

%Properties of water in subcritical state
        a06= 5900;
        a16= 250;
```

Appendix B - Simulink Code

```
function [sys, x0, str, ts] = sfd302(t, x, u, flag, x_init)
% sfd302 S-function version of the four state model
% This version is compatible with simulink block diagrams.
        global qr qdc qct
% Plant Parameters-----------------------------------------------------
        mt=300000; mr=100000; md=20000; Cp=650;
        Cfw=4.18; Ad= 23; Vd= 37; Vr= 37; Vdc= 11;
        Vt=Vd+Vr+Vdc;
        ke=200; Vsd0=8; beta=0.3;
        getstqc  % Properties of steam and water in saturated state
%--------------------------------------------------------------------
    if abs(flag) == 1,  % COMPUTE STATE DERIVATIVES
% State initial conditions
        Vwt = x(1);
        p = x(2);
        ar = x(3);
        Vsd = x(4);
% Controls or inputs
        Q = u(1)*1e6;  % Conversion to Watts
        qf = u(2);
        tf = u(3);
        qs = u(4)+4.8*(p-8.5);    % Correction for steam transducer
% Properties of steam and water in saturated state
        hs = a01+(a11+a21*(p-10))*(p-10);
        dhsdp = a11+2*a21*(p-10);
        rs = a02+(a12+a22*(p-10))*(p-10);
        drsdp = a12+2*a22*(p-10);
        hw = a03+(a13+a23*(p-10))*(p-10);
        dhwdp = a13+2*a23*(p-10);
        rw = a04+(a14+a24*(p-10))*(p-10);
        drwdp = a14+2*a24*(p-10);
        ts = a05+(a15+a25*(p-10))*(p-10);
        dtsdp = a15+2*a25*(p-10);
% Properties of water in subcritical state
        hf = (Cfw*tf+p*1e3/rw)*1e3;
% The model equations--------------------------------------------------
        hc = hs-hw;
        hr = ar*hs+(1-ar)*hw;
% Average steam quality volume ratio and partial derivatives
        z=ar*(rw-rs)/rs;
        av = rw/(rw-rs)*(1-(1/z)*log(1+z));
        davdar = rw/rs*((1/z)*log(1+z)-1/(z+1))/z;
        zp=(rs*drwdp-rw*drsdp)*ar/rs/rs;
        z1=(rw*drsdp-rs*drwdp)/(rw-rs)/(rw-rs);
        z2=rw/(rw-rs)*((1/z)*log(1+z)-1/(1+z))/z*zp;
        davdp=z1*(1-(1/z)*log(1+z))+z2;
% Circulation flow
        s1 =ke*(rw-rs)*Vr*av;
        qdc = sqrt(s1);
% Equations for coefficients of derivatives of state variables
```

```
        Td=600/qs;
        Vst=Vt - Vwt;
        Vwd=Vwt - Vdc - (1-av)*Vr;
        e11=rw-rs;
        e12=Vst*drsdp+Vwt*drwdp;
        e21=hw*rw-hs*rs;
        e22x=-Vt*1e6+mt*Cp*dtsdp;
        e22=Vst*(hs*drsdp+rs*dhsdp)+Vwt*(hw*drwdp+rw*dhwdp)+e22x;
        e3w=(rw*dhwdp-ar*hc*drwdp)*(1-av)*Vr;
        e3x=(rs+(rw-rs)*ar)*hc*Vr*davdp-Vr*1e6+mr*Cp*dtsdp;
        e32=((1-ar)*hc*drsdp+rs*dhsdp)*av*Vr+e3w+e3x;
        e33=(rs+(rw-rs)*ar)*hc*Vr*davdar;
        e42y=(1+beta)*ar*Vr;
        e42x=e42y*((1-av)*drwdp+av*drsdp+(rs-rw)*davdp)+Vsd*drsdp;
        e42=(rs*Vsd*dhsdp+rw*Vwd*dhwdp-Vsd*1e6+md*Cp*dtsdp)/hc+e42x;
        e43=(1+beta)*(ar*Vr*(rs-rw)*davdar);
        e44=rs;
        e=[e11, e12, 0,   0
           e21, e22, 0,   0
           0,   e32, e33, 0
           0,   e42, e43, e44];
% The right hand side of state equations
        b4=(hf-hw)*qf/hc+rs*(Vsd0-Vsd)/Td;
        b=[qf-qs ; Q+qf*hf-qs*hs ; Q-qdc*ar*hc ; b4];
% Solve linear equation for derivatives
        dx=e\b;
        qx=(rw-rs)*Vr*davdp*dx(2)+(rw-rs)*Vr*davdar*dx(3);
% Two important flows for understanding behavior
        qr=qdc-(av*drsdp+(1-av)*drwdp)*Vr*dx(2)+qx;
        qctx=rs*Vst*dhsdp+rw*Vwt*dhwdp-Vt*1e6+mt*Cp*dtsdp;
        qct=((hw-hf)*qf+qctx*dx(2))/hc;

% Step the derivatives, dx is a 4X1 vector
        sys = [dx];
%-----------------------------------------------------------------------
    elseif flag == 3,   % COMPUTE OUTPUTS
% Extract state variables
        Vwt = x(1);
        p = x(2);
        ar = x(3);
        Vsd = x(4);
% Drum level
        rs = a02+(a12+a22*(p-10))*(p-10);
        rw = a04+(a14+a24*(p-10))*(p-10);
        z=ar*(rw-rs)/rs;
        av = rw/(rw-rs)*(1-(1/z)*log(1+z));
        Vwd = Vwt-Vdc-(1-av)*Vr;
        ls=Vsd/Ad;
        lw=Vwd/Ad;
        l=lw+ls-1.0;
        sys = [l,p,lw,ls,qr,av,qdc,ar,Vwt,Vsd,qct];
%-----------------------------------------------------------------------
```

```
 elseif flag == 0,    % INITIALIZATIONS
     sizes(1) = 4;    % 4 continuous states
     sizes(2) = 0;    % 0 discrete states
     sizes(3) = 11;   % 11 outputs
     sizes(4) = 4;    % 4 inputs
     sizes(5) = 0;    % No discontinuous roots
     sizes(6) = 0;    % No direct term
     sizes(7) = 1; ts = [0,0];% Efficiency fix (see [1])
     sys = sizes';
     x0(1) = x_init(1);
     x0(2) = x_init(2);
     x0(3) = x_init(3);
     x0(4) = x_init(4);
else                  % Flags 2 or 4, not considered since we have no
     sys = [];        % discrete states. Also flag 5 is of no interest.
end;
```